DSPACE

https://dspace.org/

A field, petrographic and geochemical investigation of norite and anorthosite rocks related to the potholed Merensky Reef sub-facies at Northam Platinum Zondereinde mine, Western Bushveld Complex

Keikabile, Zanele

2025-10

University of the Witwatersrand, Johannesburg

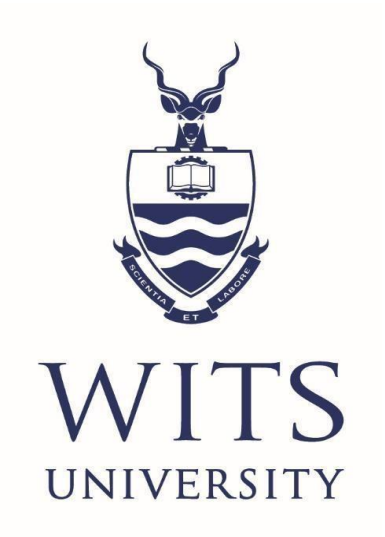
https://hdl.handle.net/10539/50300

Keikabile, Zanele. (2025). A field, petrographic and geochemical investigation of norite and anorthosite rocks related to the potholed Merensky Reef sub-facies at Northam Platinum Zondereinde mine, Western Bushveld Complex. [Master's dissertation, University of the Witwatersrand, Johannesburg]. WIReDSpace. https://hdl.handle.net/10539/50300

Downloaded from a DSpace repository. https://dspace.org/

UNIVERSITY OF THE WITWATERSRAND

JOHANNESBURG, SOUTH AFRICA



FACULTY OF SCIENCE

A field, petrographic and geochemical investigation of norite and anorthosite rocks related to the potholed Merensky Reef sub-facies at Northam Platinum Zondereinde mine, Western Bushveld Complex

Zanele Keikabile

0505994T

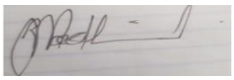
Research Report

Submitted in partial fulfilment of the requirements for the Degree of Master of Science in Economic Geology

Supervisor: Dr Ben Hayes

DECLARATION

I declare that this research report is my own, unaided work. It is being submitted for the Degree of Master of Science at the University of the Witwatersrand, Johannesburg. It has not been submitted before for any degree or examination at any other University.



(Signature of candidate)

30th day of October 2025 at Hartbeespoort

ABSTRACT

This research study is an investigation of norite and anorthosite bodies identified within potholed Merensky Reef in the southwestern extension of Northam Platinum's Zondereinde Mine, situated in the Western Limb of the Bushveld Complex, South Africa. This study aims to understand the nature and impact of these bodies on the reef as well as constrain their effect on PGE grade and mining. Data from underground geological mapping and borehole logging is combined with petrography and bulk rock trace element geochemistry. Comparisons are also made with similar norites in the hanging wall and footwall of the Merensky Reef. Underground mapping and core logging demonstrate the unpredictable spatial distribution of these bodies, with both sharp and gradational contacts being observed. Potholing and slumping of the reef also appear to be closely related to the norite-anorthosite bodies. Microstructural observations from thin sections indicate there are textural similarities between the norite bodies and the hanging wall norite to the Merensky Reef, which is also supported by the bulk rock trace element compositions. These similarities between the norite bodies and the layered stratigraphy above the Merensky Reef suggest they are connected (i.e., cogenetic) to the layered stratigraphy and they are not of an intrusive or exotic origin. The possible relationship between the norite-anorthosite bodies and Iron-Rich Ultramafic Pegmatoids is also explored, as the latter commonly replace the norite and anorthosite bodies at Zondereinde Mine. It is also shown that the norite-anorthosite bodies are barren in terms of PGE grade, and they therefore significantly dilute the PGE grades of the mined Merensky Reef, such that they pose substantial challenges to mining operations. A recommendation from this study is that there should be increased diamond drilling to better delineate the spatial distribution of these bodies. This will inform mining strategies, increase efficiency, and minimise geological losses in the southwestern extension of Zondereinde Mine.

ACKNOWLEDGEMENTS

This study was supervised by Dr. Ben Hayes, and I am sincerely grateful for his advice, guidance, critical comments, assistance with petrography and geochemical data, and patience throughout. I would also like to express my gratitude to the School of Geosciences at the University of the Witwatersrand for the opportunity to do this study and for the use of their facilities. Northam Platinum Zondereinde mine also played a critical role in allowing me to utilize the underground and geological data for this study. I am very grateful for their immense contribution in making this study possible. I am also thankful to the geology team at Zondereinde Mine for their assistance in obtaining underground photographs and samples, as well as core samples used in the study. Their dedication to great practices in ensuring detailed underground mapping and core logging greatly assisted in compiling this report. I am sincerely grateful to the lecturers for the Economic Geology courses. Special thanks to Dr. Linda Iaccheri, our course coordinator, who helped me realise that this study is possible, was always available for advice, and showed so much kindness. To the friends and acquaintances made during my MSc studies, thank you for your willingness to assist when prompted. Together, we can do so much more. Thank you to my family and friends for their support and encouragement. Special thanks to my mother, father, and husband. I embarked on this journey through the most challenging of times, but it was always my family and my faith that kept me going. All things are possible through the Lord, Jesus Christ.

TABLE OF CONTENTS

DECLARATION ..... **ii**

ABSTRACT ..... **iii**

ACKNOWLEDGEMENTS ..... **iv**

LIST OF FIGURES ..... **vii**

LIST OF TABLES ..... **xi**

1. INTRODUCTION AND BACKGROUND **1**

2. AIM OF THE STUDY **6**

2.1. Objectives 6

2.2. Context, Scope, Assumptions, and Methodology 7

3. HYPOTHESIS AND QUESTIONS **7**

4. GEOLOGICAL SETTING **8**

4.1. The Western Limb of the Bushveld Complex 10

4.2. The types of Merensky Reef at Zondereinde mine 11

4.3. The types of Merensky Reef at Northam Platinum Zondereinde Mine 13

4.3.1. Normal Merensky Reef 13

4.3.2. Regional Potholed Reef 14

5. FOCUS OF THE STUDY **15**

5.1. Norite-Anorthosite bodies 16

5.2. IRUP Replacements 19

6. METHODOLOGY **20**

6.1. Geological mapping 20

6.2. Borehole logging 20

6.3. Delineation on geological plans 20
6.4. Sample Collection 21
6.5. Petrographic analysis 22
6.6. Geochemical analysis 23
6.7. Grade analysis 24
7. RESULTS 25
7.1. Underground mapping, core logging, and delineation of the norite and anorthosite bodies 25
7.2. Petrography 28
7.2.1. Sample FW 28
7.2.2. Sample 5-10 5W-1 29
7.2.3. Sample 5-10 5W-2 32
7.2.4. Sample 9-10 4W 33
7.2.5. Sample HW 34
7.3. Whole rock geochemistry 35
7.3.1. Major Elements 35
7.3.2. Trace Elements 35
7.4. Grade analysis 40
8. DISCUSSION 42
8.1. Integrating textures, mineralogy, and trace element geochemistry 44
8.2. Origin of the norite and anorthosite bodies 47
8.3. Possible association with IRUP 48
8.4. Impact on PGE grade 49
9. CONCLUSION AND RECOMMENDATIONS 49
10. REFERENCES 51

LIST OF FIGURES

Figure 1: The spatial distribution of the major limbs comprising the Rustenburg Layered Suite, with the locations of Northam Platinum's operations indicated. Zondereinde (this study) is situated in the northern region of the Western Limb, just south of Thabazimbi (map from Northam Platinum Holdings Limited, 2024).....1

Figure 2: *A schematic cross-section showing the top of the Upper Critical Zone with the Normal Merensky Reef transgressing its footwall to form Regional Potholed Reef (after Smith & Basson, 2006).* 3

Figure 3: *The lease boundary of Zondereinde Mine, including the western extension. The distribution of the various lithofacies of PGE reefs is shown (refer to the text for details). The distribution of major dykes and faults is also indicated (map taken from Northam Platinum Holdings Limited, 2024).*.....5

Figure 4: *Anorthosite body on FWP2 horizon with the Pseudoreef harzburgite and Merensky chromitite partially replaced, and the pyroxenite hanging wall is completely replaced by the anorthosite body.*.....6

Figure 5: Simplified Stratigraphy of the Rustenburg Layered Suite (Arndt et al., 2005).....10

Figure 6: The Western Limb of the Bushveld Complex with the distribution of the Swartklip and Rustenburg Facies shown. The location of Northam Platinum Zondereinde Mine is shown in the red box. Map taken from Smith et al. (2014).....11

Figure 7*: A simplified cross-section through the Merensky Potholed Reef at Zondereinde Mine with approximate vertical distances between the different reef types indicated (figure courtesy of Zondereinde Mine). Px = Pyroxenite; Nor = Norite; Haz = Harzburgite; An = Anorthosite; Cr = Chromitite.*.....13

Figure 8*: Merensky Reef types at Zondereinde Mine with simplified 4E PGE (Platinum (Pt), Palladium (Pd), Rhodium (Rh), and Gold (Au)) grade profiles shown (photographs from Northam Platinum Holdings Limited, 2024). A) A pegmatoidal pyroxenite bracketed by two chromitite stringers with a mottled anorthosite footwall. The footwall unit is barren, with grade concentrated around the lower and upper chromite stringers. B) A single chromitite reef with grade concentrated around the chromitite. The footwall is made up of troctolite, which grades into an anorthosite layer. C) A pegmatoidal pyroxenite which is bracketed by two chromitite stringers. The grade is largely distributed throughout this sequence. The reef is underlain by*

the Upper Pseudoreef harzburgite. D) A single chromitite reef overlying the Upper Pseudoreef harzburgite with grade concentrated around the chromitite stringer. All reef types are top loaded with grade distributed 10 to 20 cm into the Merensky pyroxenite hanging wall and various degrees into the footwall. 15

Figure 9*: Anorthosite body at the elevation of the Upper Pseudoreef harzburgite at the P2/FWP2 Reef horizon. A sharp contact (orange dots) is observed between the anorthosite and the harzburgite. This picture was taken on an underground stope face at the western extension of Zondereinde Mine.* 17

Figure 10: *A) A photograph from the stope face showing the P2 reef and a leuconorite (norite body) hanging wall. The leuconorite extends into the reef and the Pseudoreef harzburgite footwall. Note the irregular contact between the chromitites and enclosed pegmatoidal pyroxenite/harzburgite as the reef ceases. The leuconorite also extends into the Pseudoreef harzburgite footwall. B) A cartoon drawing depicting an interpretation of the norite body on the stope face as shown in (A).* 18

Figure 11: IRUP with complete replacement of the country rock (photograph courtesy of Northam Zondereinde Mine).....19

Figure 12: A simplified cross-section through the Zondereinde Mine stratigraphy indicating the positions of the samples collected for this study. Smith et al. (2003) suggest there is ~72 m vertical distance between the UG-1 unit and the Bastard Reef contact.....21

Figure 13*: Field samples used for petrographic and geochemical characterisation. A) Footwall norite found below the UG1 chromitite; B) FWP2 Reef with the Merensky chromitite overlain by the norite body as its immediate hanging wall with a medium to coarse grained orthopyroxenite footwall; C) Hanging wall norite that is part of the Merensky Cyclic Unit; and D) Norite body sampled at the P2 Reef horizon with some pyroxene nodules similar to those found within the harzburgite footwall and/or pegmatoidal pyroxenite/harzburgite within the P2 Reef.* 22

Figure 14*: Samples prepared for thin sectioning. Sample 5-10 5W was divided into two samples, as observed in A and B.* 23

Figure 15: Graphical analysis of the laboratory quality control reference materials (BHVO2, BCR2, BIR1) showing the published recommended values versus the measured values.....24

Figure 16*: MicroStation diagrams showing a plan view of mined out stope faces that have intersected the norite and anorthosite bodies (grey polygons). The polygons that represent*

these bodies are up to 50 m in length. The erratic distribution of the bodies is noticeable. ...26

Figure 17*: Underground stope images of an anorthosite body at Zondereinde Mine. A) P2 Reef with anorthosite cutting through the reef and the footwall harzburgite. The anorthosite is also intrusive into the reef package with an autolith within the footwall harzburgite. B) Anorthosite overlying the Merensky chromitite (FWP2 Reef), having completely replaced the hanging wall pyroxenite. C) The anorthosite body with norite autoliths resembles a sill-like intrusion above the Merensky chromitite and partially replaces the hanging wall pyroxenite above. The P2 Reef is unaffected by this intrusion. D) The anorthosite body truncating the P2 Reef package from the hanging wall pyroxenite into footwall harzburgite, forming an irregular pothole structure with a sharp contact.*.....27

Figure 18*: Photomicrographs of sample FW under 4x magnification PPL (plane polarised light) and XPL (crossed polarised light). A) Cumulus plagioclase (plag) with interstitial orthopyroxene (opx) oikocrysts with plagioclase forming the bulk of the surrounding anorthositic matrix. B) Photomicrograph showing clinopyroxene (cpx) forming a discontinuous rim around the plagioclase. C) and D) Interstitial opx within the dominantly plagioclase-rich matrix, with minor interstitial cpx.* 29

Figure 19*: Photomicrographs of Sample 5-10 5W-1 (A, B, C, and D) under 4x magnification PPL (plane polarised light) and XPL (crossed polarised light), and reflected light images (E and F) of chromite grains (20X). A) Euhedral orthopyroxene with interstitial plagioclase. B) Abundant clinopyroxene exsolution lamellae in orthopyroxene (same field of view as A). C) and D) Interstitial clinopyroxene with chromite inclusions. E) Chromite grain from C (slightly rotated) with some sulphides also present. F) The more dominant chromite grains with highly fractured surfaces.*.....30

Figure 20: *Photomicrographs of Sample 5-10 5W-1 in reflected light. A) Chromite with interstitial sulphides along a fractured zone. B) A close-up of the sulphides along the fractured plane (20x magnification, reflected light).* 31

Figure 21: Photomicrographs of sample 5-10 5W-2 (A, B, C, D, E, F) under 4x magnification PPL (plane polarised light) and XPL (crossed polarised light). A) & B) Cumulus plagioclase with interstitial orthopyroxene and minor clinopyroxene. C) & D) Photomicrographs with minor clinopyroxene exsolution in orthopyroxene. E) Chromite within the orthopyroxene-dominant matrix at the bottom half of the sample. F) Chromite in reflected light.....32

Figure 22*: Photomicrographs of sample 9-10 4W depicting the main petrographic features under 4x magnification PPL (plane polarised light) and XPL (crossed polarised light). A) & B) Noritic phase of the sample with plagioclase, orthopyroxene and minor clinopyroxene with*

discontinuous rims around the orthopyroxene. C) & D) The leuconorite phase of the sample with dominant cumulus plagioclase and interstitial orthopyroxene. E) & F) Exsolution lamellae of clinopyroxene in orthopyroxene. 33

Figure 23: Photomicrographs of sample HW depicting the main petrographic features under 4x magnification PPL and XPL. A) Anhedral orthopyroxene with interstitial plagioclase. B) Clinopyroxene with minor exsolution lamellae as well as discontinuous rims around plagioclase. C) & D) Subhedral orthopyroxene with interstitial plagioclase and clinopyroxene. 34

Figure 24*: A graph representing the Primitive Mantle normalised patterns for the samples in the study. Note that sample 5-10 5W-1 has higher concentrations of trace elements compared to the other samples, except for Ba, La, Sr and Eu.*.....38

Figure 25: A graph representing chondrite-normalised REE patterns for the samples analysed in this study. Note that sample 5-10 5W-1 has a distinctively flatter profile and a minor negative Eu anomaly compared to the other samples.....39

Figure 26*: A scatter plot of Ce/Yb versus Ti (ppm). The Ce/Yb ratio represents the enrichment of LREE relative to HREE.*.....39

Figure 27*: A waterfall chart representing how the dilution from the norite body affected the face grade at shaft-1. The face grade decreases significantly to 2.25 g/t from a planned grade of 8.63 g/t. The major contributor is the dilution caused by the grade of the norite body at 5.02 g/t from the assayed grade of 7.27 g/t.* 41

Figure 28*: A waterfall chart representing how the dilution from the norite body affected the face grade at shaft-2. The face grade decreases significantly to 2.13 g/t from a planned grade of 7.05 g/t. The major contributor is the dilution caused by the norite body at 4.53 g/t from an assayed grade of 6.66 g/t.* 42

Figure 29*: A diagram by Maier et al. (2016) illustrating how the anorthosite pothole at Smokey Hills formed.* 44

LIST OF TABLES

Table 1*: Trace element concentration data for the five samples analysed in this study.*.....37

Table 2*: Assayed values for the reef and norite body at shaft-1.* 40

Table 3*: Shaft-1 stope planned face grade and the assayed face grade. Note that the dilution caused by the barren norite body has affected the final face grade, reducing it from an initial assayed value of 7.27 g/t to 2.25 g/t. This equates to a 69% dilution.*.....40

Table 4*: Assayed values for the reef and norite body at shaft-2* 41

Table 5: Shaft-1 stope planned face grade and the assayed face grade. Note that the dilution caused by the barren norite body has affected the final face grade, reducing it from an initial assayed value of 6.66 g/t to 2.13 g/t. This equates to a 68% dilution.....41

1. INTRODUCTION AND BACKGROUND

Northam Platinum's Zondereinde Mine is a division of Northam Platinum Holdings Limited, located in the Thabazimbi district of the Limpopo Province, South Africa (Fig. 1). It is approximately 15 km northeast of Northam town, with its underground operations mining at depths greater than 2.2 km below surface. The Merensky and UG-2 (Upper Group-2) reef types are being mined at Northam for their PGE mineralisation. These reefs are part of the Swartklip facies. The Swartklip facies is in the northern parts of the Western Limb of the Bushveld Complex (BC), with the Rustenburg facies to the south. Swartklip and Rustenburg facies were recently reviewed in a study by Mitchell et al. (2019).

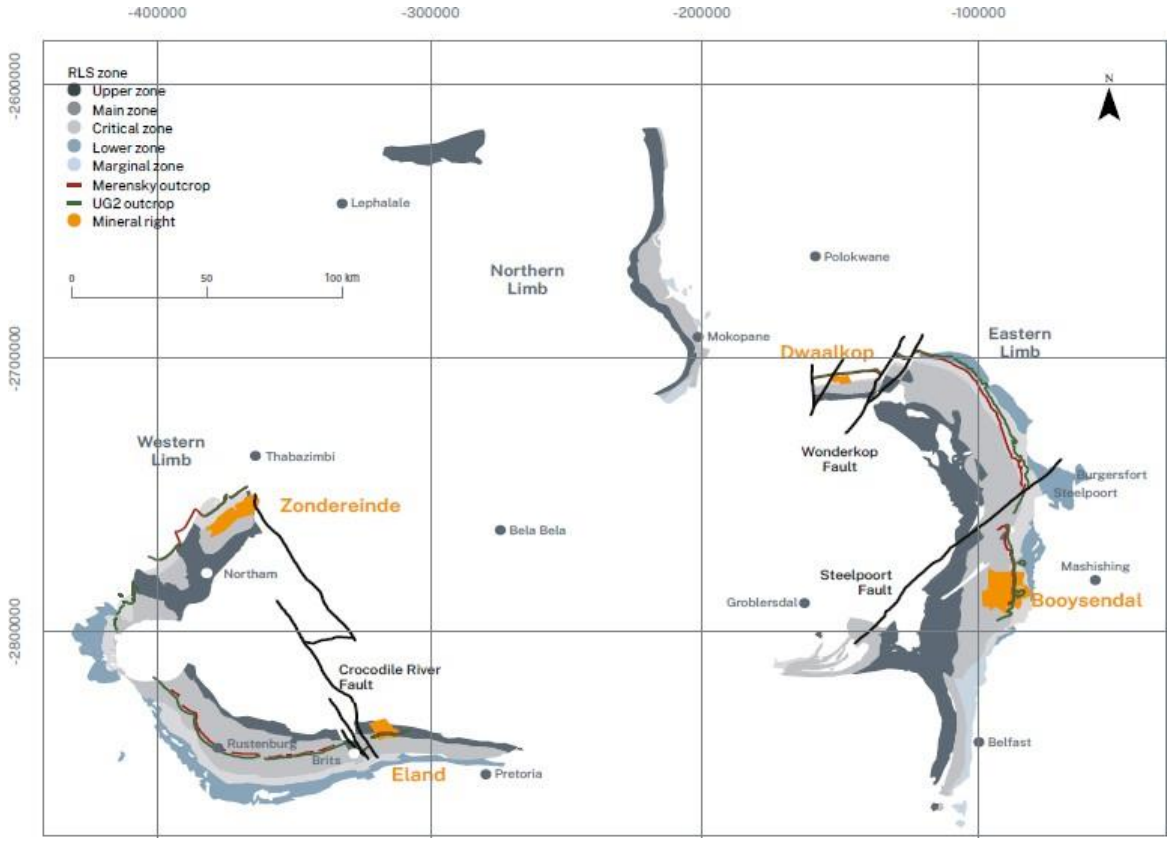


Figure 1: The spatial distribution of the major limbs comprising the Rustenburg Layered Suite, with the locations of Northam Platinum's operations indicated. Zondereinde (this study) is situated in the northern region of the Western Limb, just south of Thabazimbi (map from Northam Platinum Holdings Limited, 2024).

The Merensky and UG-2 reefs are economically exploited for their PGE (Platinum Group Elements) content in the Upper Critical Zone (UCZ) of the Rustenburg Layered Suite (RLS), with the Merensky Reef located at the base of the Merensky Cyclic Unit (MCU). The RLS is recognized as the world's largest resource of Platinum Group Elements (PGEs), and is divided

into the Upper, Main, Critical, Lower, and Marginal Zones. The MCU overlays the Merensky chromitite and grades upwards from pyroxenite at the bottom, to norite, and then anorthosite at the top (e.g., Kruger & Marsh, 1985). Above the MCU is the Bastard Cyclic Unit, which is directly beneath gabbronorite of the Main Zone.

The UG-2 Reef is approximately 14 to 38 m below the Merensky Reef at Zondereinde Mine. This interval between the two reefs is significantly thinner compared to thicknesses of up to 400 m in the Eastern Limb (Schouwstra et al., 2000; O'Connor & Alexandrova, 2021). Within this interval, however, lies the PGE-bearing Pseudoreef package with chromitite stringers (known as the Pseudoreef because it resembles the Merensky Reef in its appearance), which is accommodated between the Merensky and UG-2 reefs (Mitchell et al. 2019). The Pseudoreef is a succession of ultramafic layers with norite, anorthosite, and troctolite lithologies and may be further subdivided into Lower and Upper Pseudoreef lithologies (Fig. 2). Viring & Cowell (1999) described the Lower Pseudoreef (known as the P1 marker at Zondereinde) as an upside-down version of the Normal Merensky Reef (NMR). The NMR is present at the highest stratigraphic level (i.e., it is undisturbed or conformable), consisting of a pegmatoidal pyroxenite and pegmatoidal harzburgite, underlain and overlain by chromitite stringers, with a footwall made up of mottled anorthosite (Kinnaird, 2005). Beneath the P1 marker, which is a 1 cm chromitite stringer, lies a pegmatoidal feldspathic pyroxenite and/or pegmatoidal feldspathic harzburgite. The P1 marker is overlain by medium-grained leuconorite that grades into mottled anorthosite (P1 anorthosite), which thins from northeast to southwest, where it eventually ceases. The Upper Pseudoreef is known to locally transgress the P1 anorthosite. It consists of an irregular chromitite stringer, which is overlain by a poikilitic feldspathic dunite and/or feldspathic harzburgite, with the upper parts of this unit locally comprising orthopyroxenite, as noted by Mitchell et al. (2019). Overlying the Upper Pseudoreef is the P2 Cyclic Unit, which consists of the P2 chromitite (an approximately 2 cm chromitite stringer), overlain by a harzburgite layer, a pyroxenite layer, and a 1 cm thick anorthosite stringer termed the P2 hangingwall marker. The P2 Cyclic Unit locally transgresses (potholes) into the dunite of the Upper Pseudoreef (Viring & Cowell, 1999). Above the P2 Cyclic Unit, a 12 to 20 m thick sequence of norite, leuconorite, and anorthosite is present. This sequence leads up to the MCU, which overlies the NMR (Fig. 2).

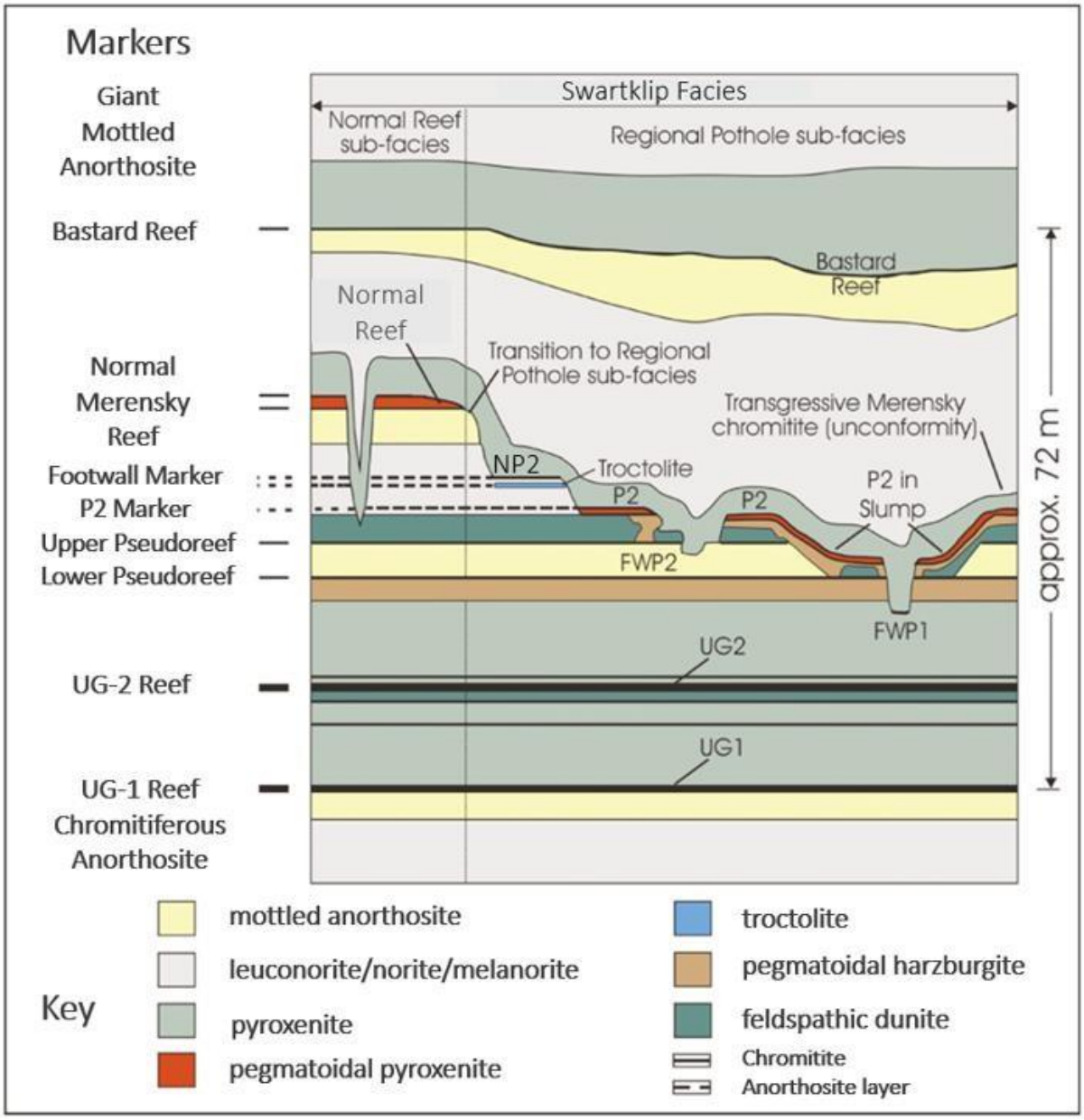


Figure 2: *A schematic cross-section showing the top of the Upper Critical Zone with the Normal Merensky Reef transgressing its footwall to form Regional Potholed Reef (after Smith & Basson, 2006).*

In places where the MCU steeply transgresses the basal chromitite stringer of the NMR and cuts the footwall lithology amidst depressed features of various scales (Hunt et al. 2018), “Potholed” Merensky Reef, known as Regional Potholed Reef (RPR), is formed. RPR is subdivided into NP2, P2, FWP2, and FWP1 reef types at Zondereinde Mine (Fig. 2). These reef types are all characterised by the composition and nature of their footwall (Smith & Basson, 2005). NP2 Reef type occurs approximately 15 m below the NMR, where the MCU overlies the footwall marker within the lower footwall units (Viring & Cowell, 1999). P2 Reef type is conformable to the Upper Pseudoreef, and FWP2 Reef type occurs where the MCU

transgresses the Upper Pseudoreef. FWP1 Reef type occurs where the MCU transgresses the Lower Pseudoreef (Fig. 2). All these reef types, except for FWP1, are economically exploited for PGE at Zondereinde Mine.

The lithostratigraphy of the Merensky Reef at Zondereinde Mine is relatively uniform. However, there are challenges related to mining. These challenges include the nature of the transitions from one reef type to another. A transition zone is defined as the area where the Merensky chromitite transgresses the footwall units into other reef types. There is a transition zone from the NMR to the NP2 Reef and vice versa, as well as from the NP2 Reef to the P2 Reef and vice versa. Transition zones are relatively steep, making them difficult to mine, which leads to geological loss. There are also mining challenges associated with the undulating NP2 Reef, the small-scale transition from P2 Reef potholing into the FWP2 Reef, and the undulating FWP2 Reef, which affects the stability of the reef. Furthermore, slumping of the reef is also a concern. Besides the challenges mentioned above, Iron-Rich Ultramafic Pegmatoids (IRUP) at Zondereinde Mine partially or completely replace the host rocks. These IRUPs further complicate mining the reef and may result in PGE losses.

In the newly acquired western extension in the southwestern portion of the mine (Fig. 3), where P2 and FWP2 Reef types within the RPR are being exploited, bodies of norite and anorthosite have been observed. These norite and anorthosite bodies appear to completely replace the reef where they are intersected, and they seem to be erratic in their spatial occurrence as they are intersected randomly by drill cores as mining progresses. The origin, structure, and lithological relationships of these norite and anorthosite bodies, as well as their effect on the face grade, are yet to be established. They are therefore the focus of this study.

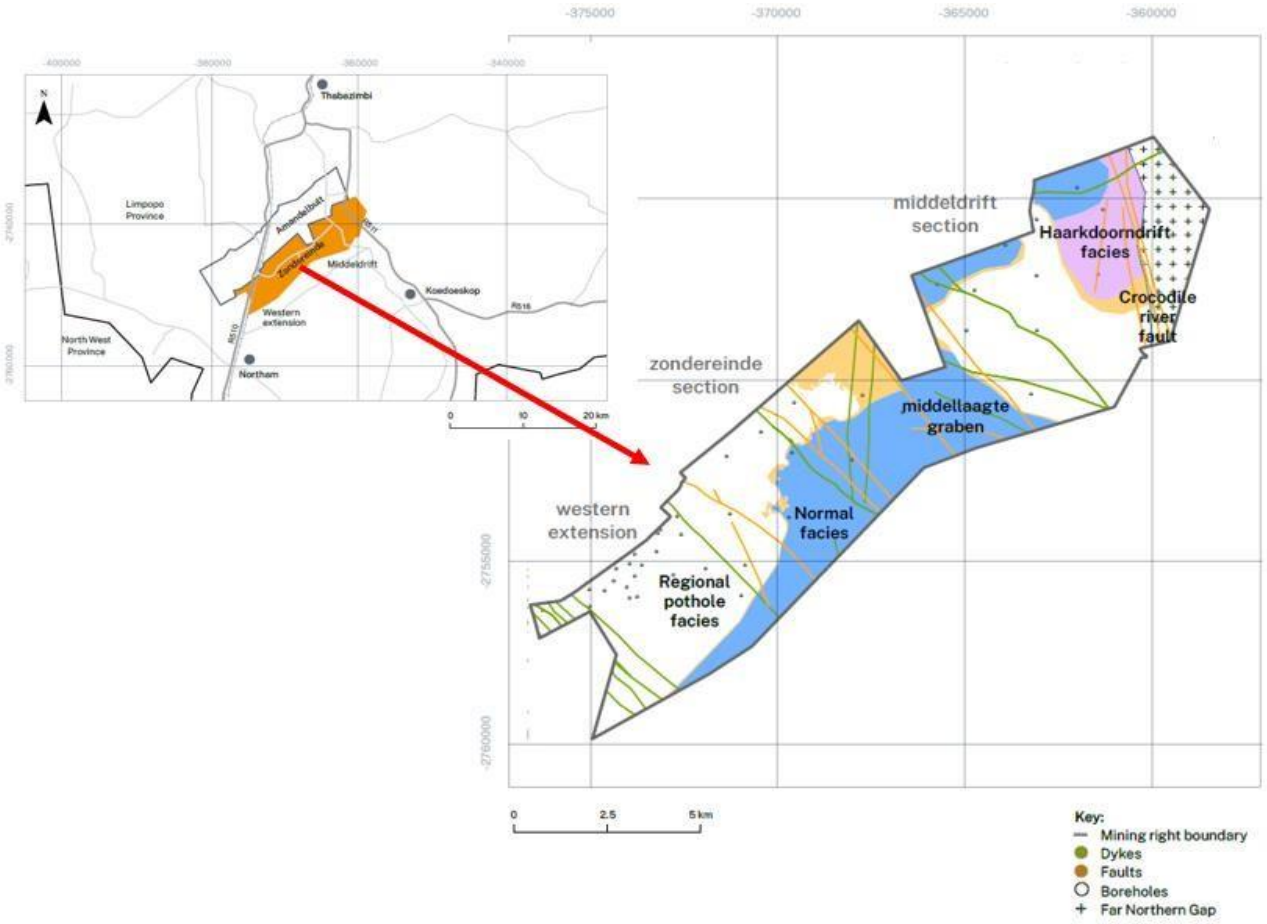


Figure 3: *The lease boundary of Zondereinde Mine, including the western extension. The distribution of the various lithofacies of PGE reefs is shown (refer to the text for details). The distribution of major dykes and faults is also indicated (map taken from Northam Platinum Holdings Limited, 2024).*

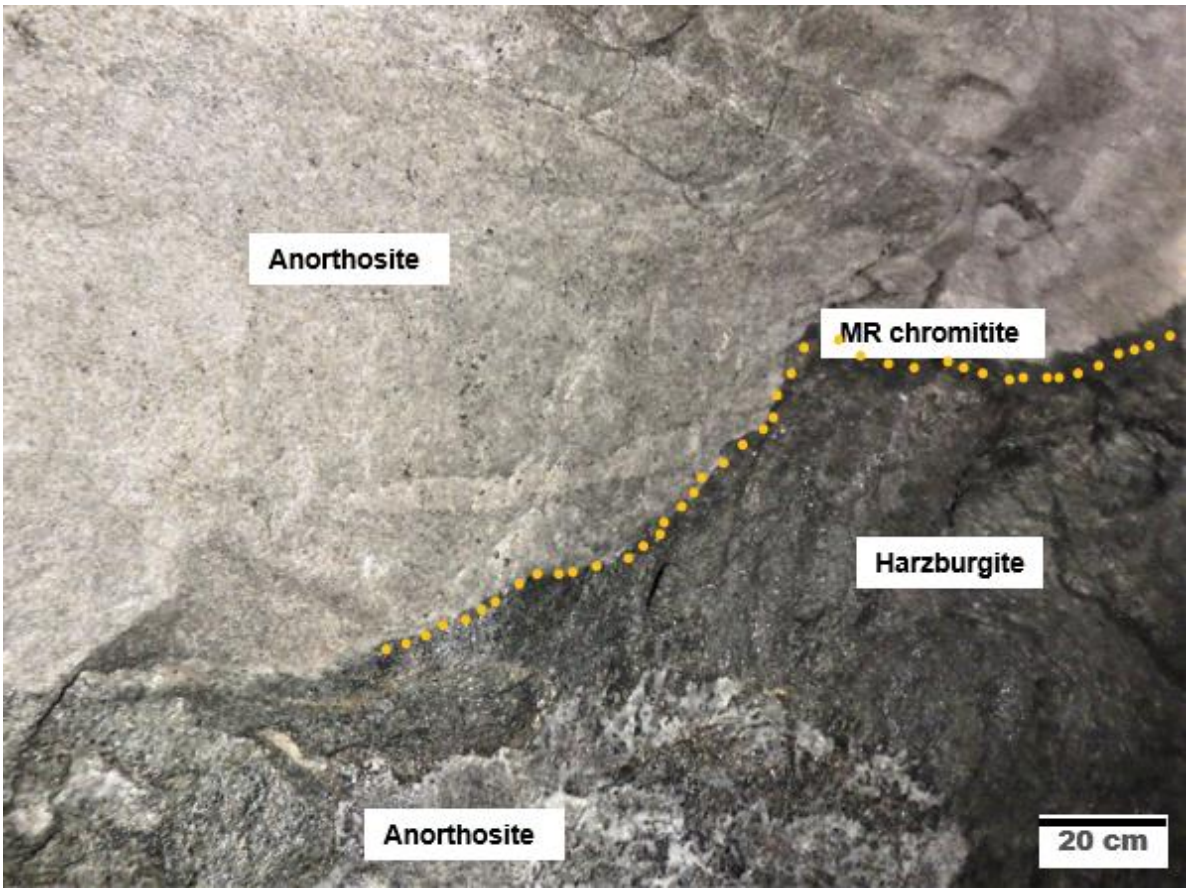


Figure 4: *Anorthosite body on FWP2 horizon with the Pseudoreef harzburgite and Merensky chromitite partially replaced, and the pyroxenite hanging wall is completely replaced by the anorthosite body.*

2. AIM OF THE STUDY

This study aims to examine and understand the nature of the abundant norite and anorthosite bodies identified in the potholed Merensky Reef at the southwestern extension of Northam Platinum Zondereinde Mine. It seeks to provide constraints regarding their impact on mining and evaluate their effect, such as dilution, on the grade of the reef. Understanding how these bodies affect the grade will ultimately determine the viability of the southwestern extension for mining and inform a mining strategy that is economical for the block of ground.

2.1. Objectives

- To determine how the norite-anorthosite bodies fit into the magmatic stratigraphy at Zondereinde Mine, which will help in understanding the origin of these bodies within

the reef horizon.

- To determine the contact relations and size variation of the bodies, to understand whether they are pothole structures or of an intrusive nature, and to deduce the extent to which they affect the orebody.
- To determine if the bodies have any association with the prevalent IRUPs that are present at the mine, as IRUP is quite prevalent within the western extension of the mine, and has been observed within the norite-anorthosite bodies.
- To establish whether these norite-anorthosite bodies are related to major potholing within the Merensky Reef or if they are isolated features. This will assist with short-term planning to avoid waste mining as norite and anorthosite are known to be barren.
- To address how these norite-anorthosite bodies affect the PGE grade of the Merensky Reef (i.e., is there any dilution).

2.2. Context, Scope, Assumptions, and Methodology

The study is conducted using information gathered from Zondereinde Mine (Northam Platinum) in the context of the known stratigraphy of the Western Limb of the Bushveld Complex. Methods used to meet the objectives include, but are not limited to, the review of geological plans, logged boreholes, underground mapping, petrography, and ICP-MS data. Limitations and uncertainties of the methods and their effect were considered.

3. HYPOTHESIS AND QUESTIONS

The sporadic nature of the norite and anorthosite bodies found within the P2 and FWP2 reef horizon (Figs. 2 & 4) at Zondereinde Mine suggests that these units may either be late, cross-cutting intrusions or a replacement product associated with the IRUP. Sharp contacts have been identified that may suggest the norite-anorthosite bodies are intrusive in origin, but this needs to be tested in further detail. In addition, petrological and geochemical information from the norite-anorthosite bodies was collected and compared with data from published literature of ‘typical’ norites that comprise the footwall and hanging wall to the Merensky Reef. Furthermore, the effect of the norite-anorthosite bodies on the PGE grade was assessed. Norites and anorthosites are known to be relatively barren in terms of PGE mineralisation; therefore, when they are intersected within the reef, this will result in dilution and thus affect

the face grade[1] and possibly the milling head grade[2]. The face grade assists with immediate information for operational decision making, short-term planning, and the reduction of mining costs by focusing on good-quality ore. The milling head grade focuses on the overall feasibility of the mining operation, efficiencies of the processing plant, and comparing predicted grades with actual production. This study examines how the extent of these barren bodies impacts grade and daily mining operations when reef markers are completely replaced. blending

4. GEOLOGICAL SETTING

The Bushveld Complex in South Africa has been dated between 2060 and 2055 Ma (Scoates et al., 2021) and is composed of broadly four concurrent components. The Rustenburg Layered Suite (RLS) is a shallow-dipping layered sequence of mafic to ultramafic rocks. It is overlain by approximately 1.5 to 4 km of granite, which includes the Rashoop Granophyre and the Lebowa Granite Suite (Kleemann & Twist, 1989; Hill et al., 1996; Kinnaird et al., 2004). The Rooiberg Group is a volcanic succession that precedes the RLS intrusion of the Bushveld Complex (Lenhardt & Eriksson, 2012). The Lebowa and Rashoop granites are believed to have intruded into the roof of the RLS and the felsic rocks of the Rooiberg Group (Eriksson et al. 1995; Naldrett et. al., 2011). The RLS was emplaced into the Transvaal Supergroup and the Rooiberg Volcanic Suite (Eriksson et al., 1995; Viljoen, 2016). The RLS is exposed at the surface in five major limbs: Eastern, Western, Far Western, Northern, and Southeastern (Fig. 1).

The RLS, extending over ~100,000 km², is the largest mafic-ultramafic layered intrusion on Earth (Cawthorn, 2015). The magmatic stratigraphy of the RLS has been divided into the Upper, Main, Critical, Lower and Marginal Zones (Fig. 3). Characteristically, the Upper Zone has a sequence of banded gabbros as well as several magnetite-rich layers, with the location of the main vanadium-rich magnetite layer being near the base of the Upper Zone (Cawthorn & Walraven, 1998; Willmore et al., 2000; Kinnaird, 2005; Viljoen, 2016). The Main Zone constitutes nearly half of the RLS thickness. The lower part of this zone is characterised by gabbronorite with more pyroxenite present in the upper part (Kinnaird, 2005; Naldrett et. al., 2011). The Critical Zone is characterised by layering of mafic-ultramafic cumulate rocks (Schoenberg et al., 1999). It is divided into the Lower Critical Zone (LCZ), which is entirely ultramafic, comprising a succession of pyroxenite cumulates with numerous chromitite layers,

Footnotes

[1] *Face grade: measured directly at the exposed mining face using channel sampling.*

[2] *Milling head grade: weighted average grade of ore entering the processing plant (mill) after mining, transportation, blending, and possible dilution with waste.*

and the Upper Critical Zone (UCZ), with regularly rhythmically layered chromitite, pyroxenite, anorthosite, norite, and locally some more olivine-rich rocks (e.g., harzburgite and troctolite) (Schoenberg et al., 1999; Kinnaird, 2005; Yudovskaya et al., 2013; Viljoen, 2016). The chromitites in both subzones of the Critical Zone are of economic value – some being exploited for chromium, and others for PGE (Willmore et al., 2000). The repeated sequences of the Critical Zone are known as cyclic units (a well-documented one being the Merensky Cyclic Unit (MCU)). There may be layers of chromitite at the base of the cyclic units, which are relatively rich in PGEs compared to the surrounding rocks (Schoenberg et al., 1999). The well-documented Merensky Reef and UG- 2 chromitite are in the UCZ (Latypov et al., 2015). The Lower Zone is not well exposed, with the best outcrops located in the northern regions of the Eastern and Western Limbs (Kinnaird, 2005). It consists mostly of pyroxenitic rocks as well as local layers of harzburgite and dunite (Cawthorn & Walraven, 1998; Viljoen, 2016). The Marginal Zone has limited exposure, with thicknesses ranging from zero to a few metres at outcrops. It primarily consists of quartz and biotite-bearing norite and pyroxenite (Cawthorn & Walraven, 1998; Kinnaird, 2005).

The RLS is known to host the greatest concentrations of magmatic ore deposits on Earth that are rich in chromium, vanadium, and platinum-group metal (PGM) resources. PGMs are largely contained in the Merensky Reef, UG-2, and Platreef (Arndt et al., 2005; Osbahr et al., 2014).

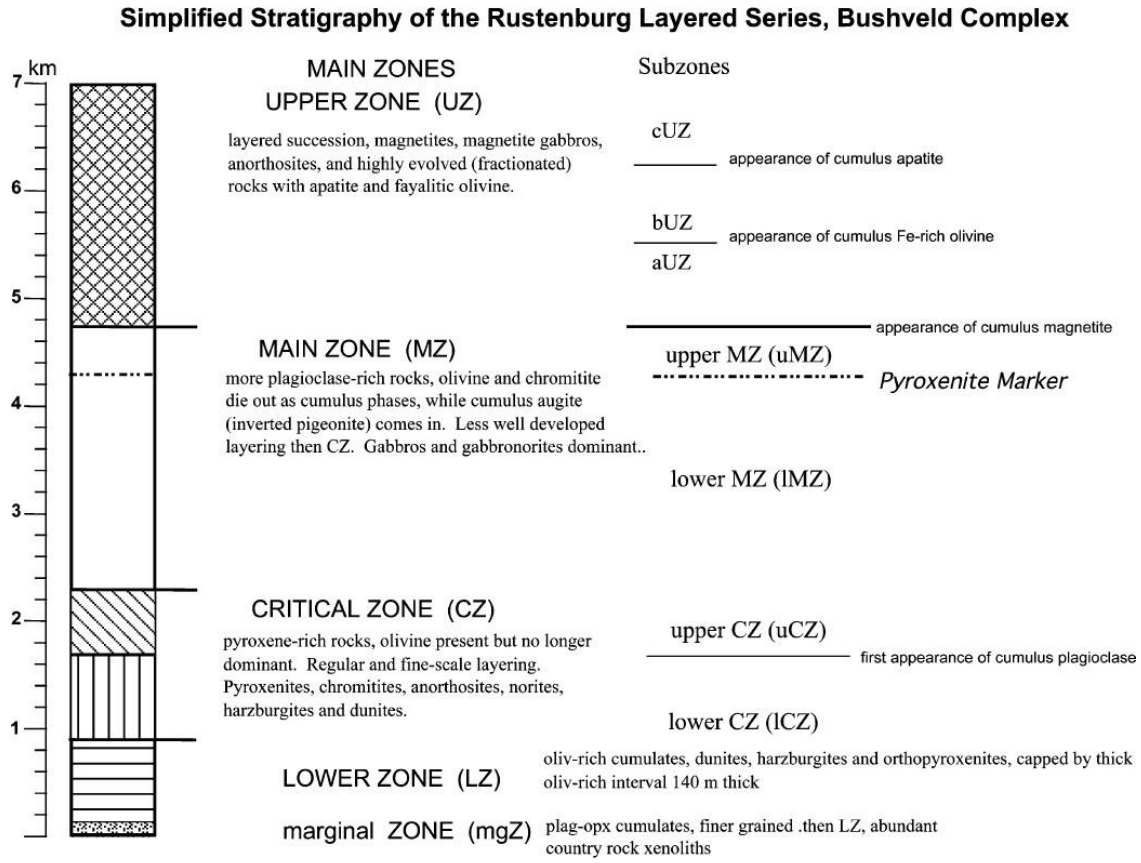


Figure 5: Simplified Stratigraphy of the Rustenburg Layered Suite (Arndt et al., 2005)

4.1. The Western Limb of the Bushveld Complex

A major lithofacies subdivision has been proposed for the Western Limb of the Bushveld Complex. The northern regions of this limb are made up of Swartklip facies, whereas the southern regions are made up of Rustenburg facies (e.g., Viljoen, 1999; Mitchell et al., 2019). The boundary between these two lithofacies subdivisions is considered to be located around the significantly younger Pilanesberg alkaline complex (Fig. 6). The Critical Zone of the Swartklip facies shows stratigraphic thinning below the level of the Merensky Reef (Viring & Cowell, 1999; Mitchell et al., 2019). This includes thinned sequences of plagioclase-rich rocks intercalated with the Merensky and UG- 2 Reefs as compared to thicker sequences of plagioclase-rich rocks in other parts of the RLS (Mitchell et al., 2019). Additionally, the ultramafic rocks between the Merensky and UG-2 Reefs in the Swartklip facies contain the 3 to 5 m thick Pseudoreef unit, which is rich in olivine (Mitchell et al., 2019). Potholing is present in both the Rustenburg and Swartklip facies. While the Swartklip facies has larger potholes, with most mining activities conducted in potholed facies types, the Rustenburg facies has smaller potholes that have a comparatively minor impact on mining activities (Smith et al., 2013). The Normal Merensky Reef and the Regional Potholed Merensky Reef are the two

subfacies commonly mined in the Swartklip facies. The Regional Potholed Reef is divided into three high-grade reef facies types and one low-grade non-economic facies type. Eleven reef facies types have been identified from the multiple varied facies within the Rustenburg facies (Moodley, 2008); however, there are four main subfacies, namely, the high-grade narrow, pegmatoidal, and potholes reef types as well as the low-grade, sub-economic non-pegmatoidal reef type (Viljoen, 1999).

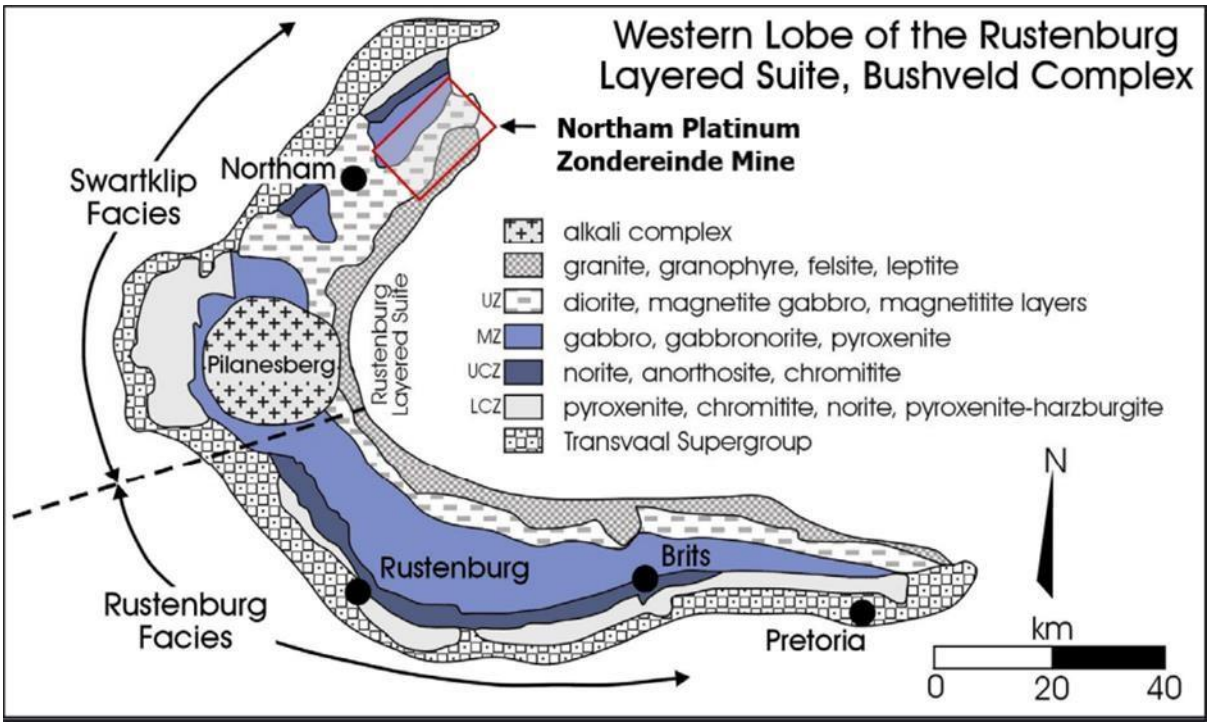


Figure 6: The Western Limb of the Bushveld Complex with the distribution of the Swartklip and Rustenburg Facies shown. The location of Northam Platinum Zondereinde Mine is shown in the red box. Map taken from Smith et al. (2014).

4.2. The types of Merensky Reef at Zondereinde mine

At Zondereinde Mine, the Merensky Reef has been classified as either Normal Merensky Reef or Regional Potholed Reef (Reid & Basson, 2002). Potholes are described as areas where the MCU has transgressed the basal chromitite of the Normal Merensky Reef, resulting in irregularities that form transgressive contacts with footwall lithology (Smith & Basson, 2005, 2006; Becker et al., 2011; Latypov et al., 2017a; Hunt et al., 2018; Chistyakova et al., 2019). This is where “Potholed” Merensky Reef, also known as Regional Potholed Reef (Reid & Basson, 2002), is formed (Fig. 6). Potholing, prevalent in the Swartklip facies, is attributed to thermochemical erosion by replenishing magmas during the formation of the Bushveld Complex, resulting in basin-shaped depressions forming within potholed reefs (Latypov et al., 2015; 2017a; 2022). To create a functional categorisation scheme for the mining sector, the

Merensky Reef has been classified into different facies, sub-facies, and reef types (Reid & Basson, 2002).

Reef types within the RPR are identifiable where the Merensky Reef becomes conformable to footwall cumulates (Roberts et al., 2006) and are therefore characterised by the nature of their footwall. NP2 Reef type occurs where the Merensky Reef is conformable to the footwall marker and is approximately 12 to 15 m below the NMR (Viring & Cowell, 1999). The upper transition from NMR to NP2 Reef is known as the first order of potholing. P2 Reef type occurs where the Merensky Reef is conformable to the Upper Pseudoreef and is approximately 5 m below the NP2 Reef. The lower transition from NP2 Reef, together with P2 Reef, is termed the second order of potholing (Viring & Cowell, 1999). FWP2 Reef type occurs where the Merensky Reef transgresses the Upper Pseudoreef into harzburgite and/or dunite below or into the Lower Pseudoreef anorthosite (Smith & Basson, 2006). The non-exploited FWP1 Reef type occurs where the Merensky Reef transgresses the Lower Pseudoreef. FWP2 and FWP1 Reefs are the deepest and lowest order of potholing, termed the third and fourth order, respectively (Viring & Cowell, 1999).

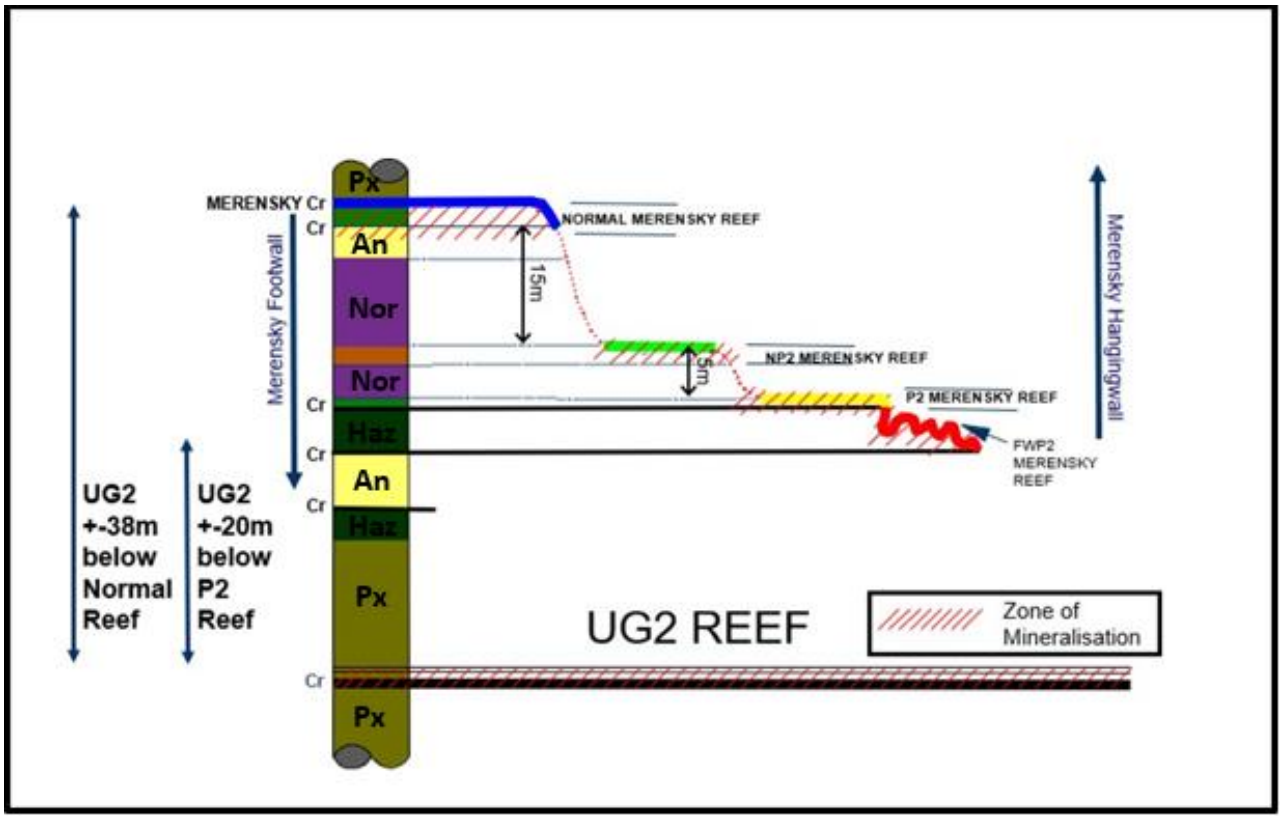


Figure 7*: A simplified cross-section through the Merensky Potholed Reef at Zondereinde Mine with approximate vertical distances between the different reef types indicated (figure courtesy of Zondereinde Mine). Px = Pyroxenite; Nor = Norite; Haz = Harzburgite; An = Anorthosite; Cr = Chromitite.*

4.3. The types of Merensky Reef at Northam Platinum Zondereinde Mine

4.3.1. Normal Merensky Reef

The NMR facies at Zondereinde Mine is present at a higher stratigraphic level of the Upper Critical Zone, with no transgression of its footwall (Roberts et al., 2006; Figs. 2 & 7). The NMR comprises a layer of massive dunite, pegmatoidal harzburgite, and pegmatoidal pyroxenite (Smith et al., 2003), collectively bracketed by chromite stringers. The average thickness of the NMR as observed at Zondereinde is 3 m. The top chromite stringer (Merensky chromitite) forms the base of the MCU, being overlain by a hanging wall composed of a medium-grained poikilitic to feldspathic pyroxenite (Smith et al., 2003). At the base of the NMR is a chromite stringer, which overlies a mottled anorthosite footwall. The NMR gradually thins as the reef begins to transgress its footwall and approach the edge of the RPR sub-facies (Roberts et al., 2006; Figs. 2 & 7).

4.3.2. Regional Potholed Reef

The Regional Potholed Reef is subdivided into different classes, depending on the composition of the footwall unit upon which the reef sits. Each class is summarised here.

NP2 Reef

Transitioning steeply from NMR into the footwall cumulates, the NP2 Reef overlies a sequence of the footwall rocks consisting of anorthosite and leuconorites to melanorites (Reid & Basson, 2002; Figs. 2 & 7). At Zondereinde, NP2 Reef is located 10 to 20 m below the upper chromite stringer of the NMR, with the inter-reef thickness varying from the eastern to the western quadrant of the mine, with thinning observed towards the west. The footwall to the NP2 Reef consists of a 5 to 50 cm thick layer of anorthosite, with a variable troctolite layer that grades into underlying anorthosite or a leuconorite to melanorite (Fig. 8B).

P2 Reef

Transitioning steeply from the NP2 Reef, the P2 Reef is in proximity to an anorthosite stringer (1–2 cm thick) termed the “P2 hanging wall marker” at the top of the P2 Cyclic Unit. It is at this stratigraphic level that the MCU is underlain by a pegmatoidal pyroxenite and/or harzburgite (Reid & Basson, 2002; Figs. 2 & 7). This is underlain by the P2 chromitite, which overlies the medium-grained Upper Pseudoreef harzburgite and/or dunite (Reid & Basson, 2002; Roberts et al., 2006; & Becker et al., 2011; Fig. 8C).

FWP2 Reef

The FWP2 Reef occurs in areas where the MCU transgresses the Upper Pseudoreef harzburgite and/or dunite. Its footwall is a dunite and/or harzburgite (Fig. 8D). Where deep potholing occurs, FWP2 overlies the Lower Pseudoreef anorthosite. At this level, FWP2 Reef also locally transgresses deep into the footwall to the Lower Pseudoreef pegmatoidal harzburgite to form the FWP1 Reef type (Fig. 2). Historically, due to its undulating nature, FWP2 Reef was not targeted for mining; however, it is now being successfully mined together with P2 Reef types in the western portion of Zondereinde Mine, where disruptions are less common.

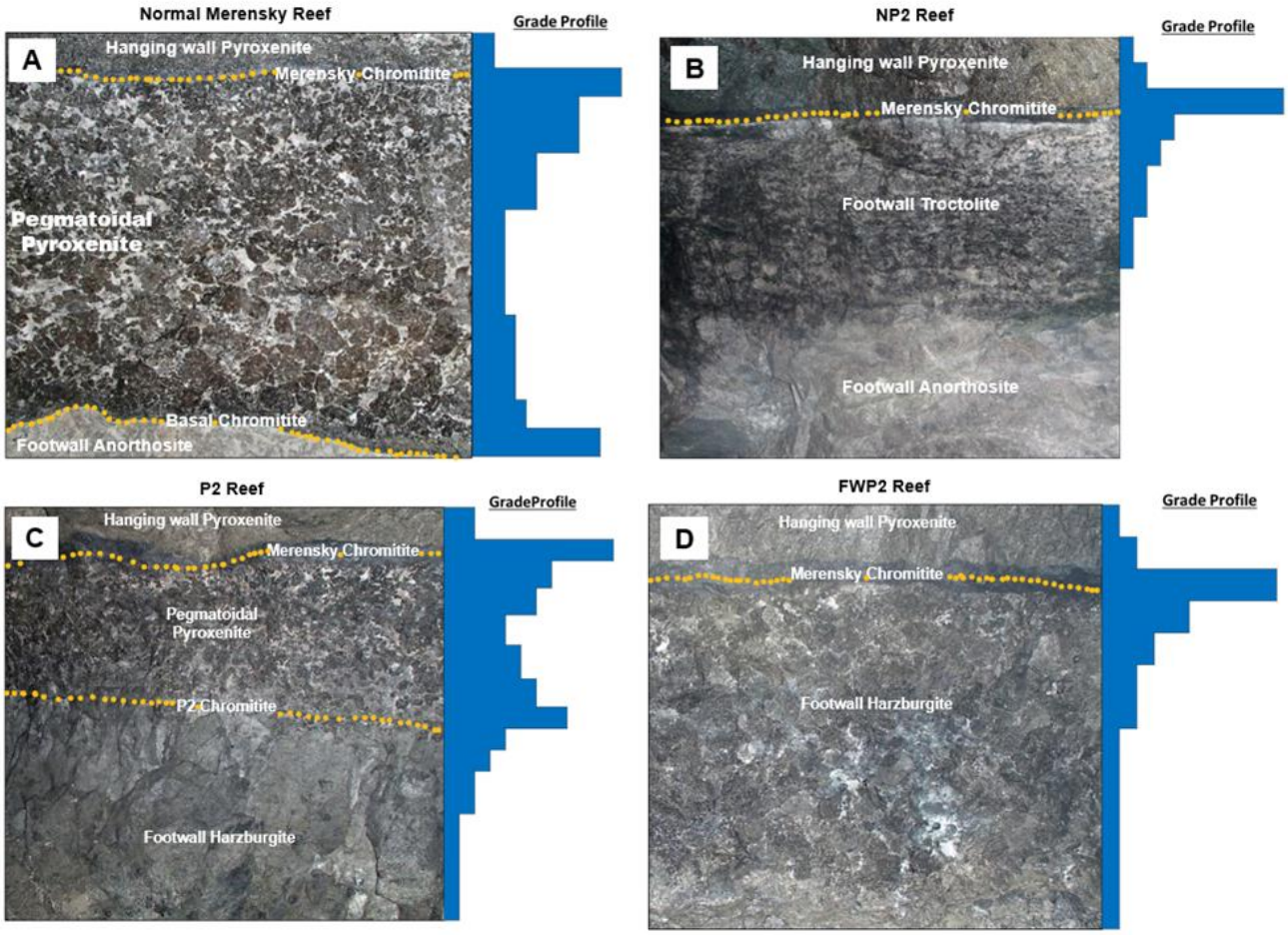


Figure 8*: Merensky Reef types at Zondereinde Mine with simplified 4E PGE (Platinum (Pt), Palladium (Pd), Rhodium (Rh), and Gold (Au)) grade profiles shown (photographs from Northam Platinum Holdings Limited, 2024). A) A pegmatoidal pyroxenite bracketed by two chromitite stringers with a mottled anorthosite footwall. The footwall unit is barren, with grade concentrated around the lower and upper chromite stringers. B) A single chromitite reef with grade concentrated around the chromitite. The footwall is made up of troctolite, which grades into an anorthosite layer. C) A pegmatoidal pyroxenite which is bracketed by two chromitite stringers. The grade is largely distributed throughout this sequence. The reef is underlain by the Upper Pseudoreef harzburgite. D) A single chromitite reef overlying the Upper Pseudoreef harzburgite with grade concentrated around the chromitite stringer. All reef types are top loaded with grade distributed 10 to 20 cm into the Merensky pyroxenite hanging wall and various degrees into the footwall.*

5. FOCUS OF THE STUDY

This study focused on the area where the Regional Potholed Reef is being mined at the south-western region of Zondereinde Mine, in the western extension, where P2 and FWP2 Reef

types are being exploited. Norite and anorthosite bodies, together with IRUP, are prevalent in this area.

5.1. Norite-Anorthosite bodies

Norite and anorthosite bodies are prevalent in the western extension at Zondereinde Mine. These norite and anorthosite bodies have not been studied, but appear to be associated with regional potholing (Figs 4 & 10). There have also been assumptions that these bodies may be associated with IRUPs, which are also prevalent in the western extension. The norite-anorthosite bodies appear to completely replace and/or intrude the host rock and the reef horizon where they occur (Fig. 9 & 10). They are erratic, and their source/origin is currently unknown. Mitchell et al. (2019) have, however, noted that in the Amandelbult enclave (northwest of the Swartklip facies where Northam Zondereinde and Anglo-American's Platinum Amandelbult Mines are situated), the UG-2 hangingwall pyroxenite and the Pseudoreef contain thin norite and/or anorthosite units. They mentioned that the harzburgite of the Pseudoreef unit also appears to be intercalated with these norite and/or anorthosite units. While these authors noted these units, there is no detailed information regarding their nature. At Zondereinde Mine, the norite and anorthosite bodies either show sharp contacts (Fig. 9) or irregular contacts (Fig. 10), and they appear to be related to the hanging wall units, cutting through the footwall stratigraphy, thereby affecting the typical layered sequence.

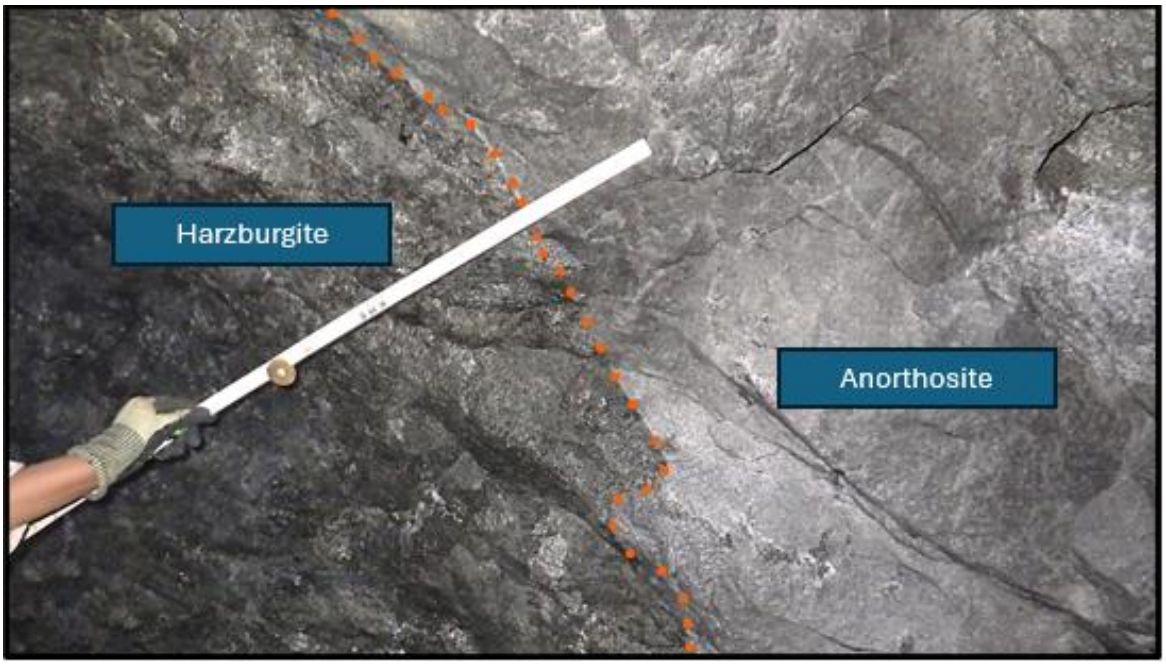


Figure 9*: Anorthosite body at the elevation of the Upper Pseudoreef harzburgite at the P2/FWP2 Reef horizon. A sharp contact (orange dots) is observed between the anorthosite and the harzburgite. This picture was taken on an underground stope face at the western extension of Zondereinde Mine.*

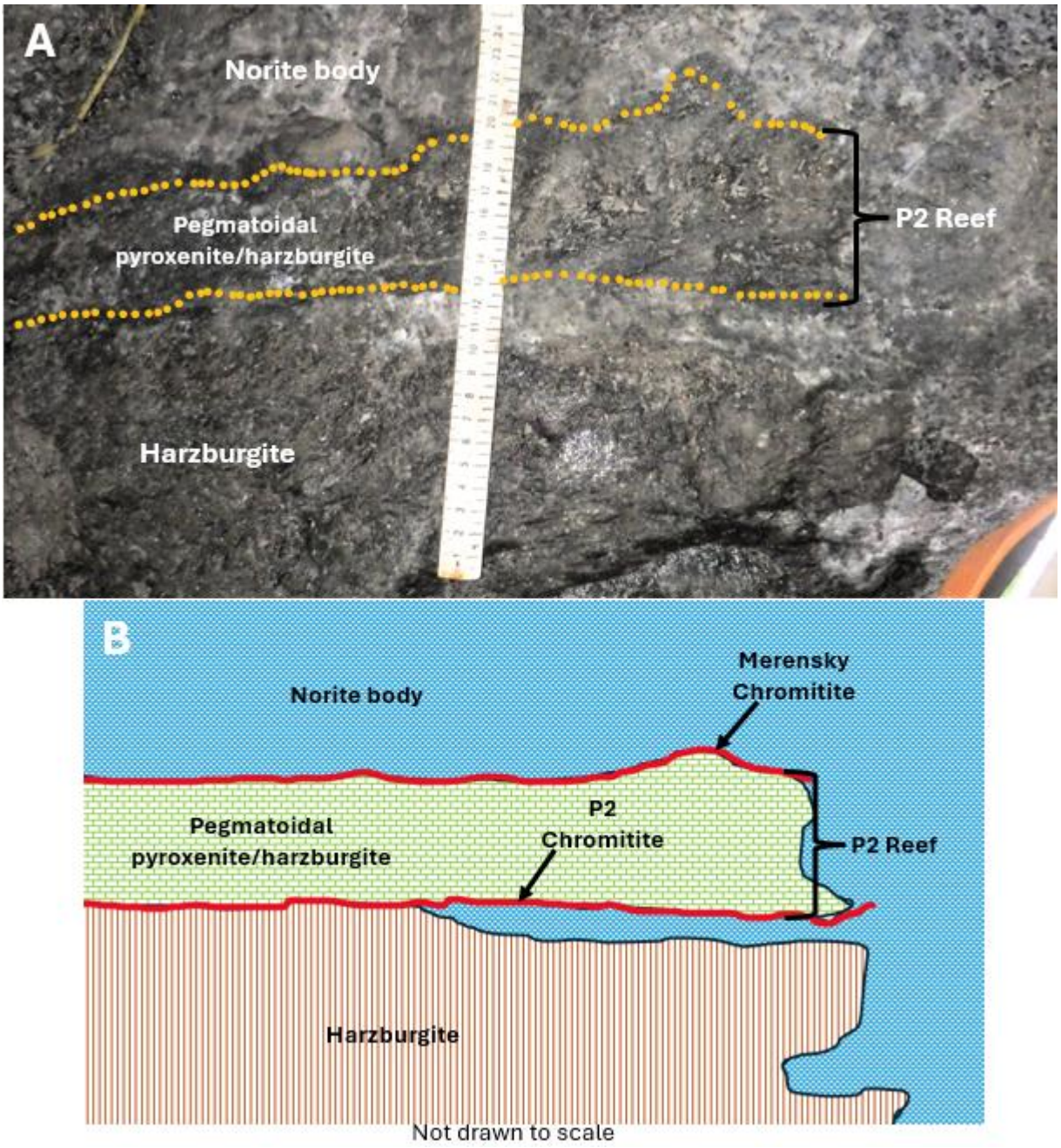


Figure 10: *A) A photograph from the stope face showing the P2 reef and a leuconorite (norite body) hanging wall. The leuconorite extends into the reef and the Pseudoreef harzburgite footwall. Note the irregular contact between the chromitites and enclosed pegmatoidal pyroxenite/harzburgite as the reef ceases. The leuconorite also extends into the Pseudoreef harzburgite footwall. B) A cartoon drawing depicting an interpretation of the norite body on the stope face as shown in (A).*

5.2. IRUP Replacements

IRUPs are prevalent in the western extension at Zondereinde Mine and have been observed in proximity to the norite and anorthosite bodies that are investigated in this study. This spatial association may suggest that the IRUPs are related to the norite-anorthosite bodies. IRUPs are a hindrance to mining as they partially or completely replace the reefs and the surrounding country rocks. IRUPs are commonly present in the UCZ of the RLS, particularly within the Merensky Reef and UG-2 orebodies (Zhou et al., 2023). At the Lonmin Karee Mine, IRUP primarily replaces anorthosite and pyroxenite, and extends from the footwall of the UG2 chromitite to the Main Zone (Zhou et al., 2023). Similar occurrences of IRUP have been observed at Zondereinde Mine, with IRUP extending from beneath the UG1 chromitite up to the Main Zone.

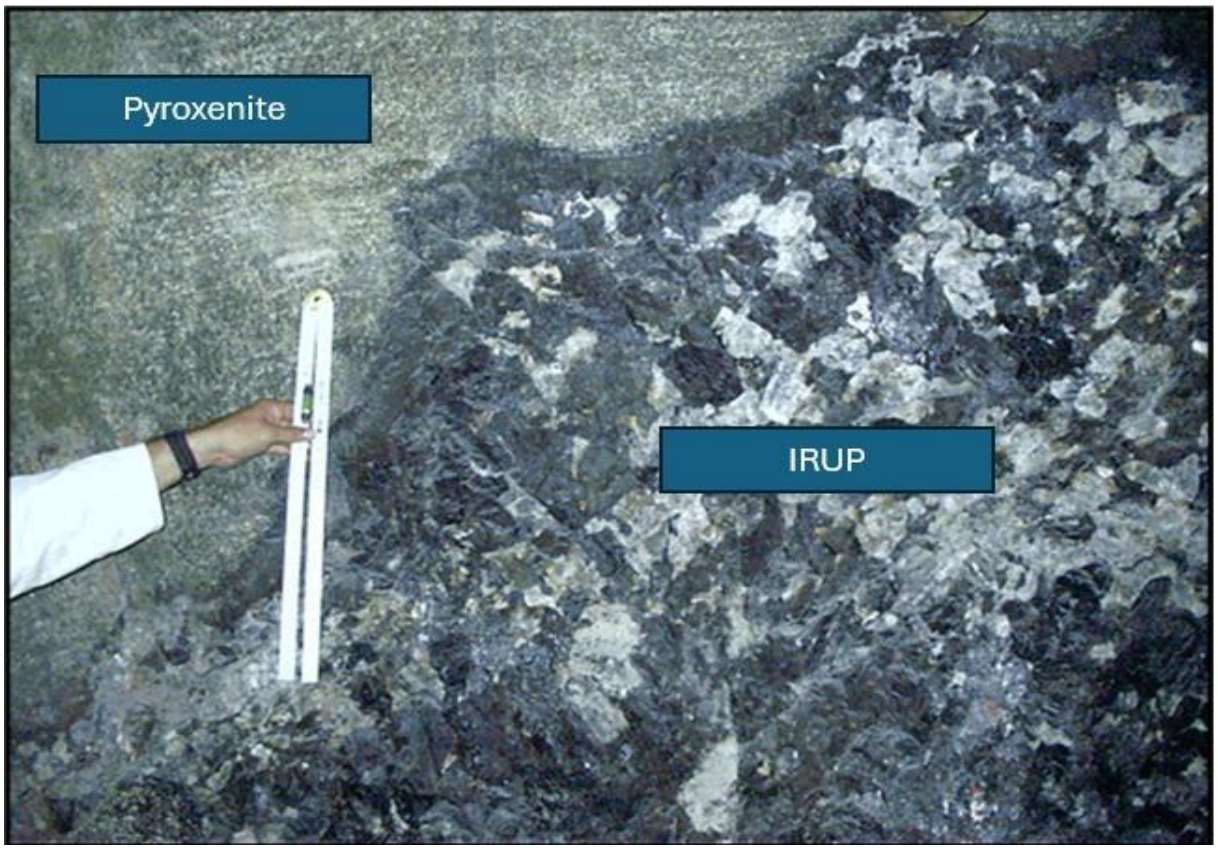


Figure 11: IRUP with complete replacement of the country rock (photograph courtesy of Northam Zondereinde Mine).

6. METHODOLOGY

6.1. Geological mapping

Underground mapping is continuously conducted by the geology team at Zondereinde Mine. Mapping is done at least every 5–10 m of blasting advance (i.e., at least twice a month), except in areas where the norite and anorthosite bodies affect more than 50% of the stope face, where there is prevalence of IRUPs, and where off-reef mining is observed, mapping is conducted at least once a week. Mapping is conducted to continuously assess the lithology exposed on the stope face for grade control and to assess ground conditions affected by geological discontinuities (i.e., faults, dykes, etc.). The geological maps produced are plotted on plans and used for interpretations of lithofacies, geological losses, geological modelling, using polygons for the different reef facies, and IRUP. Polygons of the norite-anorthosite bodies have recently been added for this study and will be used to determine their extent on the stope faces.

6.2. Borehole logging

An underground diamond drilling programme is being conducted at Zondereinde Mine to establish the continuity of the reefs at a local scale. These boreholes are logged by the geology team, and intersections of norite and anorthosite bodies have been noted within the P2 Reef horizon in the study area. In boreholes, where the norite and/or anorthosite bodies are observed, no reef has been intersected. These bodies have been matched with underground mapping within the same vicinity.

6.3. Delineation on geological plans

All mapping and borehole data at Zondereinde Mine are plotted on the mine's geological plans. These include survey plans as well as digital MicroStation plans. These plans are used for the interpretation of underground mapping and borehole data, where reef polygons are created and continuously monitored for use in geological loss estimations as well as resource and reserve estimations. For this study, polygons of the norite-anorthosite bodies were created and updated on the digital plans as underground mapping is updated and borehole data is interpreted. These polygons will assist with determining the approximate sizes of these bodies as they are intersected. The norite and anorthosite bodies are indicated as one unit on the plan and are therefore not separated into different polygons.

6.4. Sample Collection

In December 2023, four field samples were taken from different stratigraphic levels at Zondereinde Mine to be used for petrographic and geochemical characterisation of the norite-anorthosite bodies (Fig. 12). Two samples (5-10 5W and 9-10 4W) were taken from underground workings (stope faces) on the reef horizon (P2/FWP2 Reef) where the norite body in question is intersected. The other two samples (FW and HW) are from underground drill core: one from norite within the footwall stratigraphy (approximately 65 m below P2 Reef) and the other from norite in the hanging wall of the MCU (approximately 3–6 m above the P2 Reef). The locations of these samples in the magmatic stratigraphy are indicated in Figure 12 below.

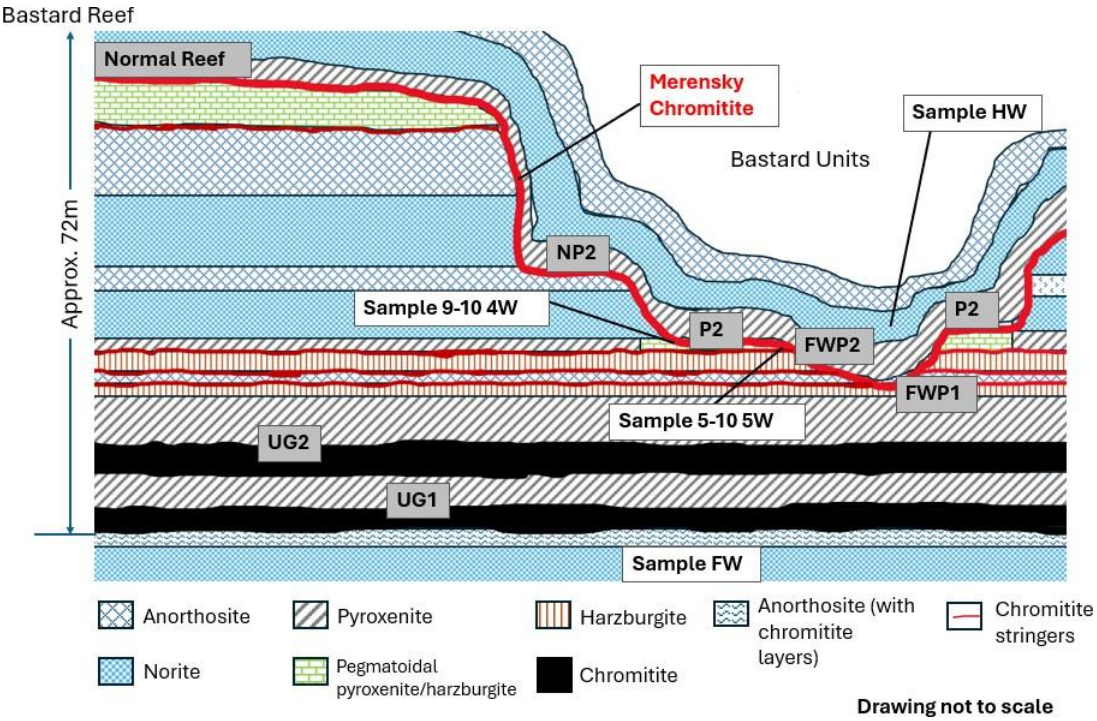


Figure 12: A simplified cross-section through the Zondereinde Mine stratigraphy indicating the positions of the samples collected for this study. Smith et al. (2003) suggest there is ~72 m vertical distance between the UG-1 unit and the Bastard Reef contact.

Sample 5-10 5W was divided into two parts, namely, sample 5-10 5W-1 and sample 5-10 5W-2. Sample 5-10 5W was of a singular chromitite stringer overlying a medium to coarse-grained orthopyroxenite, and in turn overlain by the norite body, which continues into an orthopyroxenite. The sample was divided in this way to assess the norite body as a separate sample from the chromitite and its footwall. There was, therefore, a total of five samples to be prepared for analysis.

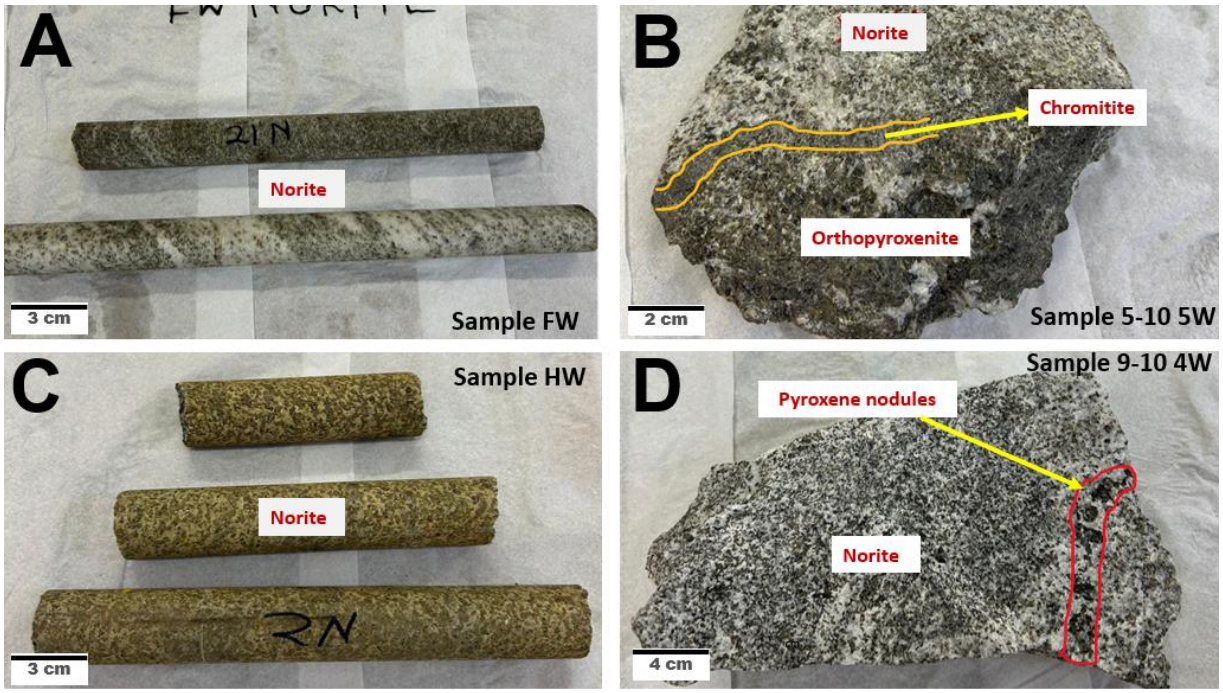


Figure 13*: Field samples used for petrographic and geochemical characterisation. A) Footwall norite found below the UG1 chromitite; B) FWP2 Reef with the Merensky chromitite overlain by the norite body as its immediate hanging wall with a medium to coarse grained orthopyroxenite footwall; C) Hanging wall norite that is part of the Merensky Cyclic Unit; and D) Norite body sampled at the P2 Reef horizon with some pyroxene nodules similar to those found within the harzburgite footwall and/or pegmatoidal pyroxenite/harzburgite within the P2 Reef.*

6.5. Petrographic analysis

The purpose of petrographic analysis was to investigate the textures in the norite bodies and compare them to the feldspathic cumulates that sit above and below the Merensky Reef in the regular stratigraphic sequence. The samples collected were taken to the University of the Witwatersrand, where they were cut into fist-sized pieces using a circular, diamond-crusted saw. A small flat chip was cut and marked clearly for thin sectioning (Fig. 14). The thin sections were studied using an Olympus BX41 optical microscope to identify the mineralogy of each sample. Full thin section images and detailed photomicrographs of the thin sections were acquired to characterise the textures in the samples.

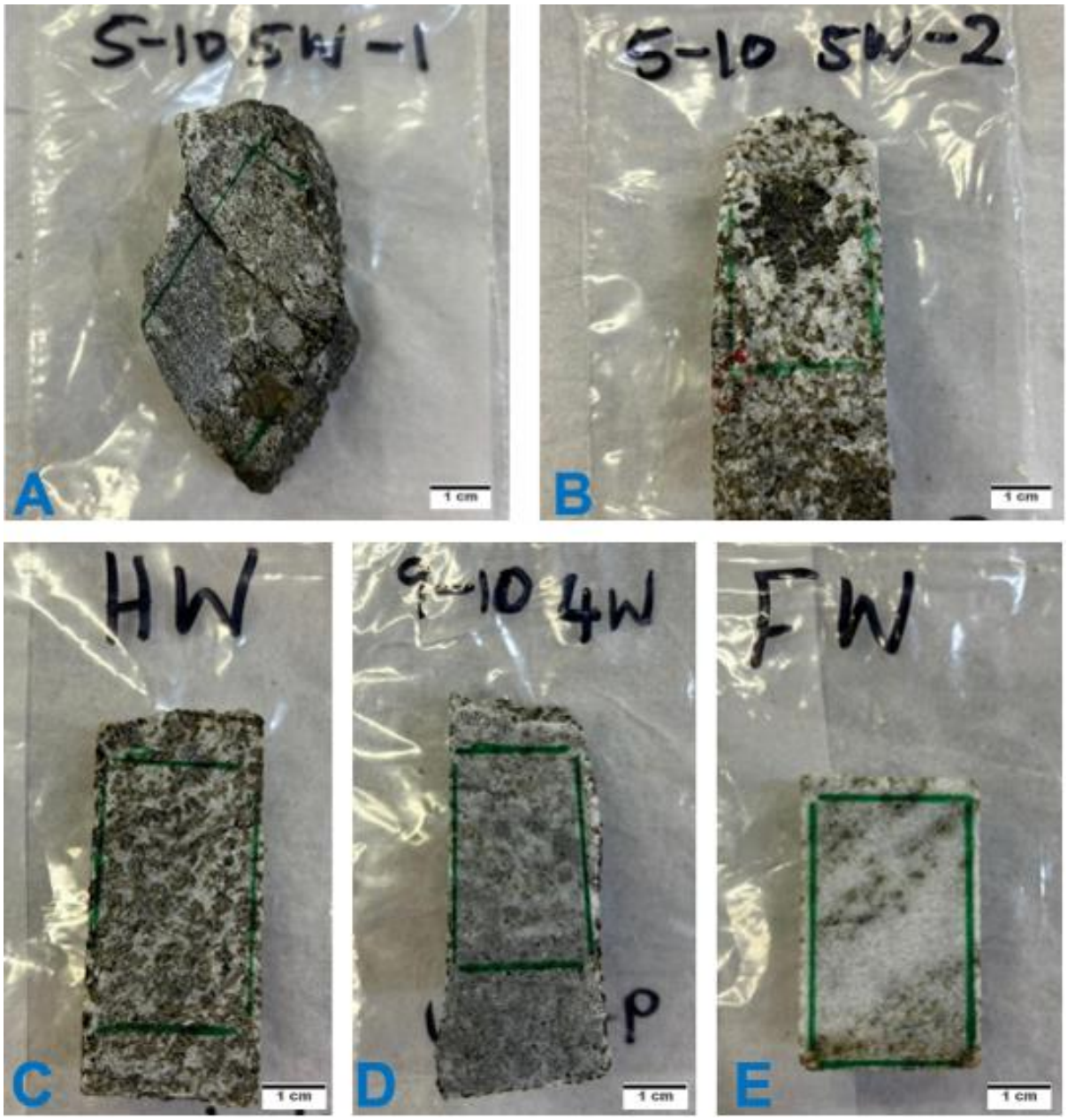


Figure 14*: Samples prepared for thin sectioning. Sample 5-10 5W was divided into two samples, as observed in A and B.*

6.6. Geochemical analysis

A fraction of the cut and washed samples was crushed and milled into a fine powder at the University of the Witwatersrand. The five powders were submitted to the Earth Observatory at the University of the Witwatersrand in February 2024 for major and trace element analysis. Due to the X-ray fluorescence (XRF) being out of service throughout 2024 and into early 2025, the major element data was not obtained during this study. The trace element data was

analysed using an inductively coupled plasma-mass-spectrometer (ICP-MS) by Marlin Patchappa.

The Earth Observatory used the reference materials BCR2 (Columbia River Basalt), BHVO2 (Hawaiian Volcano Observatory Basalt), and BIR1 (Reykjavik Iceland Basalt) for QA/QC. These are basalt materials used in laboratories globally as standard reference materials. The United States Geological Survey (USGS) has summarised mass fraction values for the elements in the reference materials from literature sources and multi-laboratory analysis. The standard reference material has been plotted against the analytes measured in the Zondereinde samples. There is a linear relationship between the recommended standard reference material used and the measured analytes, except for Ti and Sr, which plot 40% above the recommended values. These two elements are not represented in Figure 15 below.

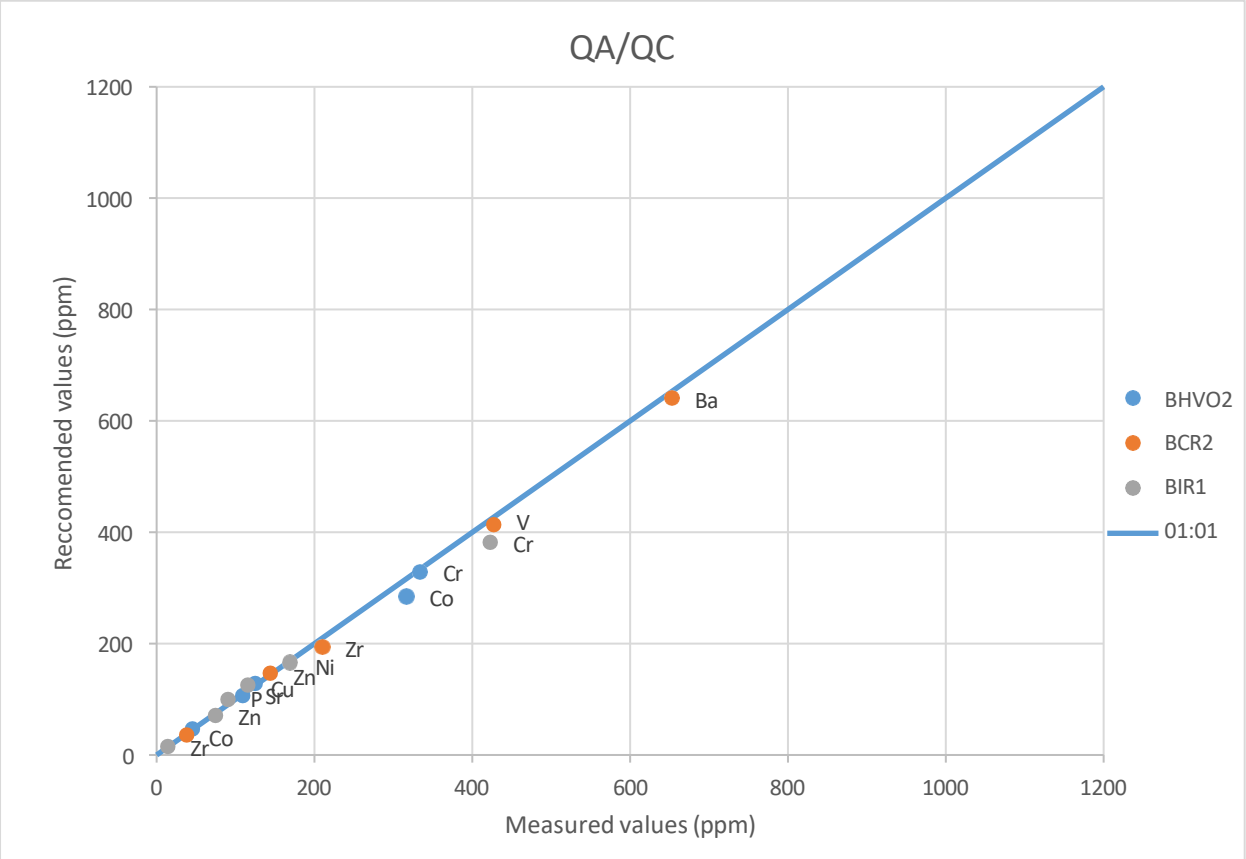


Figure 15: Graphical analysis of the laboratory quality control reference materials (BHVO2, BCR2, BIR1) showing the published recommended values versus the measured values.

6.7. Grade analysis

Sampling was conducted at the underground workings (stope faces) where the norite bodies were observed. There were two stope faces sampled (Shaft-1 and Shaft-2) that are approximately 195 m apart (vertical distance) and were both affected by the norite body. The

samples were sent to the laboratory at Zondereinde Mine for 4E (Pt, Pd, Rh, Au) analysis to determine the effect of the norite bodies on the face grade, which ultimately may affect the milling head grade. The Zondereinde laboratory uses fire assay to measure 4E data.

Regarding the data from the laboratory and from underground mapping, calculations were done to determine how the norite bodies affect the face grade at both Shaft-1 and Shaft-2. The ratio of the 4E assayed grade (a weighted average of the sample batch), the weighted average of the laboratory densities for each sample batch, and the volume of the reef channel and the norite body from the field were calculated. These parameters are used to calculate the final face grade after dilution.

7. RESULTS

7.1. Underground mapping, core logging, and delineation of the norite and anorthosite bodies

Underground mapping demonstrates that the norite and anorthosite bodies are erratically intersected on the P2 Reef horizon in the study area. This has also been noted in the underground logged diamond drill cores. These bodies have both sharp and gradational contacts at different intersections. It has been noted that no faulting is present in areas where these bodies are intersected, but potholing, as well as slumping of the reef, has been observed in some stopes, whereas in other stopes the norite bodies seem to have intruded the reef horizon and partially replaced the reef to a certain extent.

Based on mapping and core logging information, the norite-anorthosite bodies have been delineated and plotted as polygons in MicroStation. The polygon sizes range from 2 m to 50 m in radius (Fig. 16).

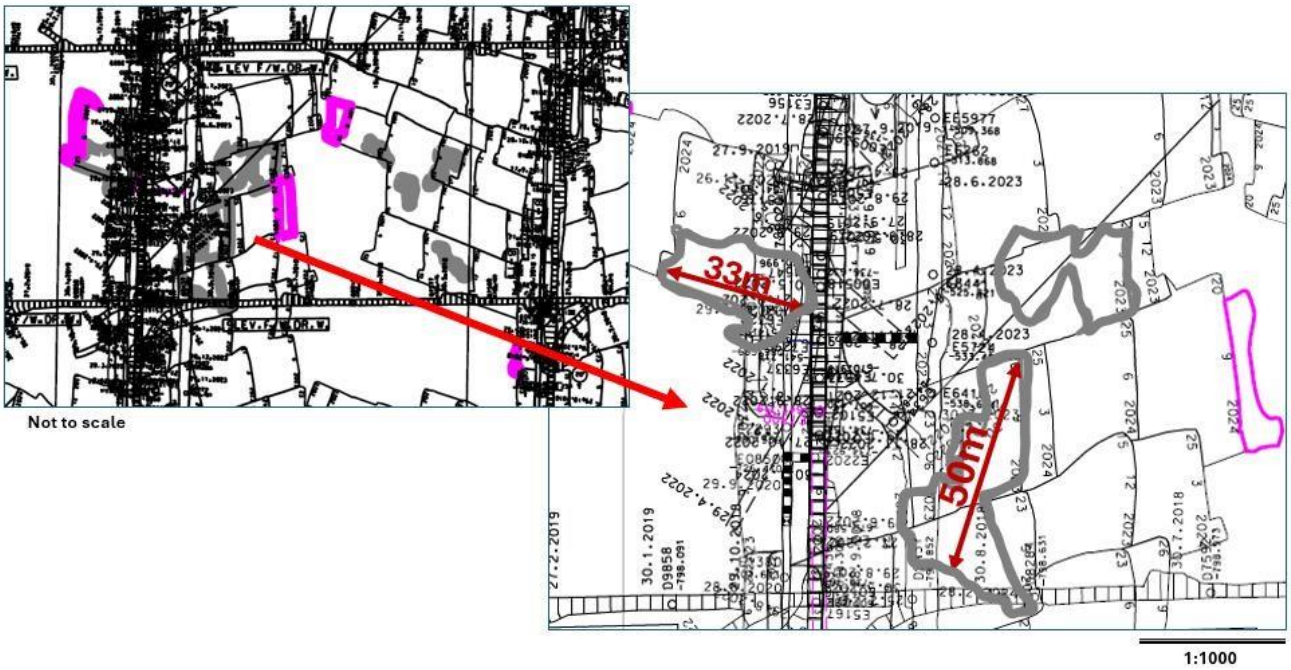


Figure 16*: MicroStation diagrams showing a plan view of mined out stope faces that have intersected the norite and anorthosite bodies (grey polygons). The polygons that represent these bodies are up to 50 m in length. The erratic distribution of the bodies is noticeable.*

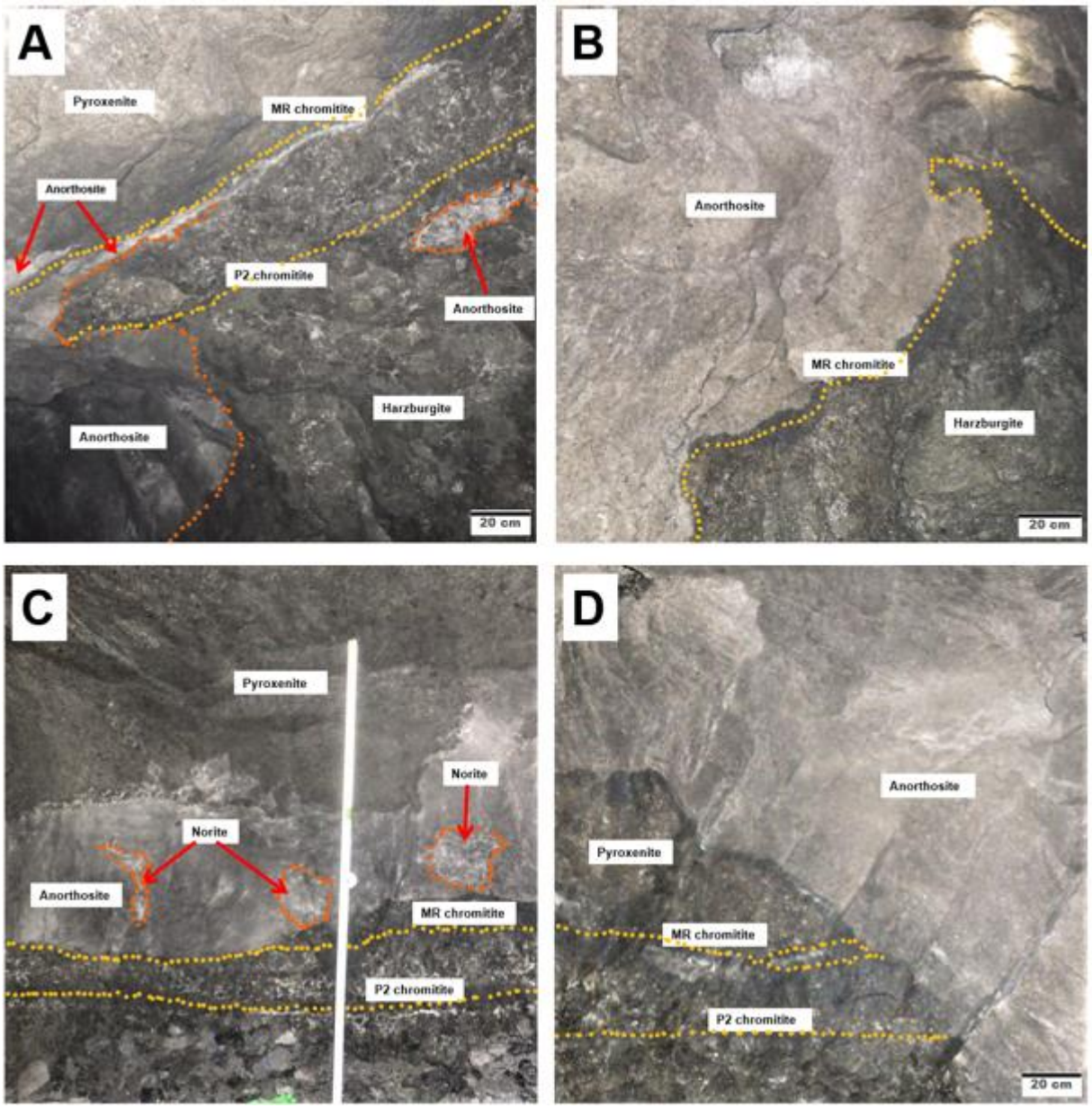


Figure 17*: Underground stope images of an anorthosite body at Zondereinde Mine. A) P2 Reef with anorthosite cutting through the reef and the footwall harzburgite. The anorthosite is also intrusive into the reef package with an autolith within the footwall harzburgite. B) Anorthosite overlying the Merensky chromitite (FWP2 Reef), having completely replaced the hanging wall pyroxenite. C) The anorthosite body with norite autoliths resembles a sill-like intrusion above the Merensky chromitite and partially replaces the hanging wall pyroxenite above. The P2 Reef is unaffected by this intrusion. D) The anorthosite body truncating the P2 Reef package from the hanging wall pyroxenite into footwall harzburgite, forming an irregular pothole structure with a sharp contact.*

IRUP was also closely observed during the underground mapping and borehole logging. The IRUP seems to have intruded and replaced the norite and anorthosite bodies in the same

manner as observed in the stratigraphy from beneath the UG-1 unit and up into the Main Zone. IRUP in this area has also been noted to pervade the Merensky Reef and surrounding ultramafic rocks. An interesting observation is that some of the IRUP sampled and assayed at Zondereinde's western extension are barren, with some areas showing relatively low grades.

7.2. Petrography

This section focuses on the macroscopic and microscopic analysis of the norite and anorthosite bodies in relation to the hanging wall and footwall cumulates within the regular magmatic stratigraphy.

7.2.1. Sample FW

Sample FW is medium-grained with areas of banded leuconorite and anorthosite, which has been colloquially termed "streepies norite" at Zondereinde Mine. Streepies refers to how the orthopyroxene-bearing layers look like stripes. It is important to note that the mineralogical composition of the norite varies within the footwall stratigraphy. In places, a melanorite is observed, and in other places, a leuconorite, which locally grades into anorthosite, is observed. Banding is quite common within the footwall stratigraphy, especially near the UG-1 chromitite. Sample FW is predominantly a plagioclase-rich adcumulate with approximately 90% plagioclase, 8% orthopyroxene, and 2% clinopyroxene. Plagioclase has a cumulus texture, whereas the orthopyroxenes and clinopyroxenes are interstitial, forming oikocrysts. Orthopyroxene oikocrysts enclose plagioclase chadacrysts that give rise to a poikilitic texture (Fig. 18A). The margins of the oikocrysts are intergrown with plagioclase laths that form the bulk of the anorthositic matrix. The less abundant clinopyroxenes occur as discontinuous rims at the edges of the cumulus plagioclase.

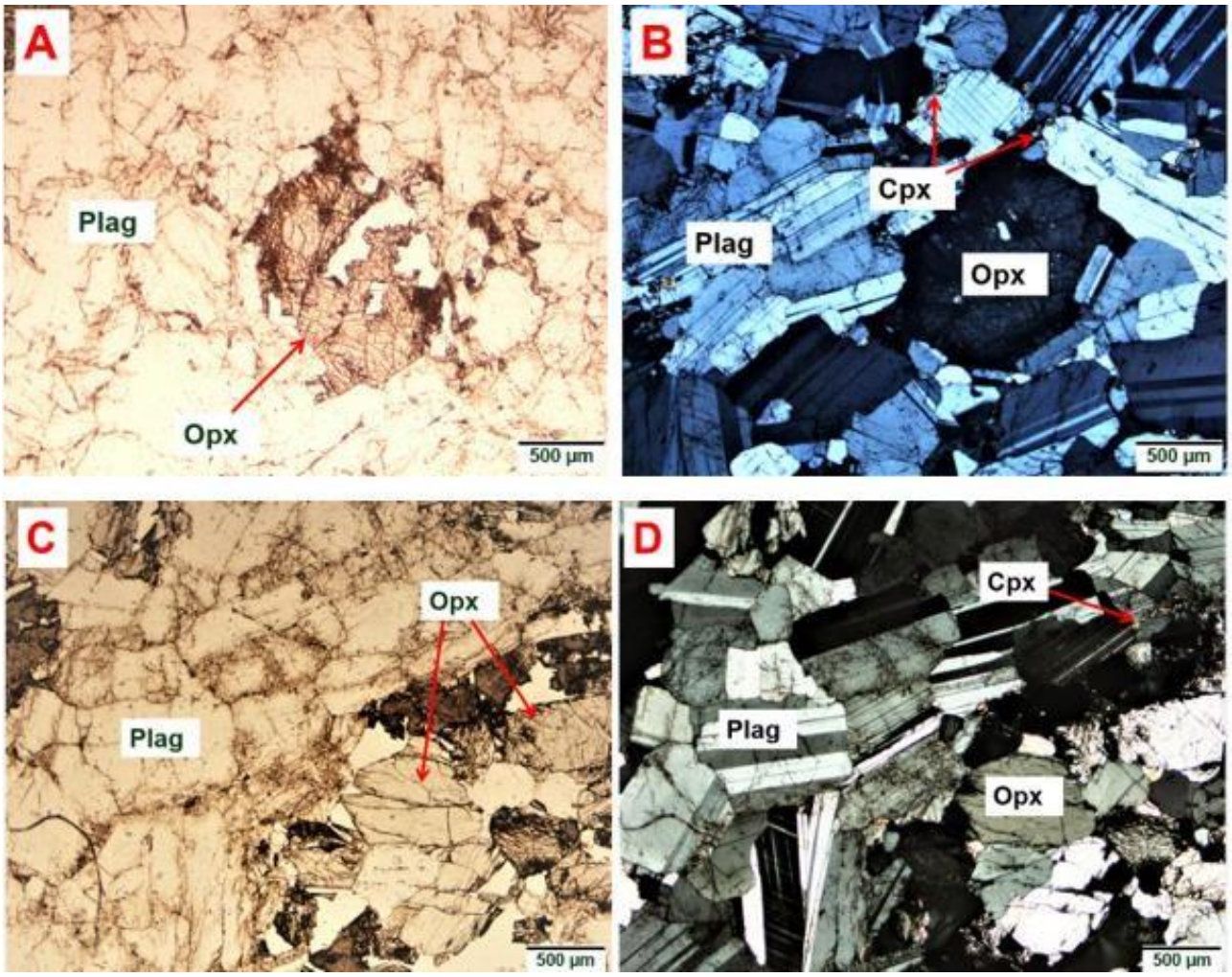


Figure 18*: Photomicrographs of sample FW under 4x magnification PPL (plane polarised light) and XPL (crossed polarised light). A) Cumulus plagioclase (plag) with interstitial orthopyroxene (opx) oikocrysts with plagioclase forming the bulk of the surrounding anorthositic matrix. B) Photomicrograph showing clinopyroxene (cpx) forming a discontinuous rim around the plagioclase. C) and D) Interstitial opx within the dominantly plagioclase-rich matrix, with minor interstitial cpx.*

7.2.2. Sample 5-10 5W-1

Sample 5-10 5W-1 is medium to coarse-grained, representing the Upper Pseudoreef harzburgite and/or orthopyroxenite. It consists of 90% orthopyroxene, 7% plagioclase and 3% clinopyroxene. The orthopyroxene is euhedral and coarse-grained, while plagioclase is interstitial and appears anhedral. The less dominant clinopyroxenes are interstitial, with exsolution lamellae of clinopyroxene in the orthopyroxene. The high birefringence streaks of the clinopyroxene lamellae within the orthopyroxene is evident in Figure 19B.

The sample contains chromite grains included within the clinopyroxene and orthopyroxene. Some of the chromite grains are euhedral, with fracturing in the more prominent chromite grains (Fig. 19F). There are intercumulus sulphides present in chromite grains along a fractured zone, as noted in Figures 19E and 20B. There is no evidence of olivine in the thin section, indicating that the sample is an orthopyroxenite.

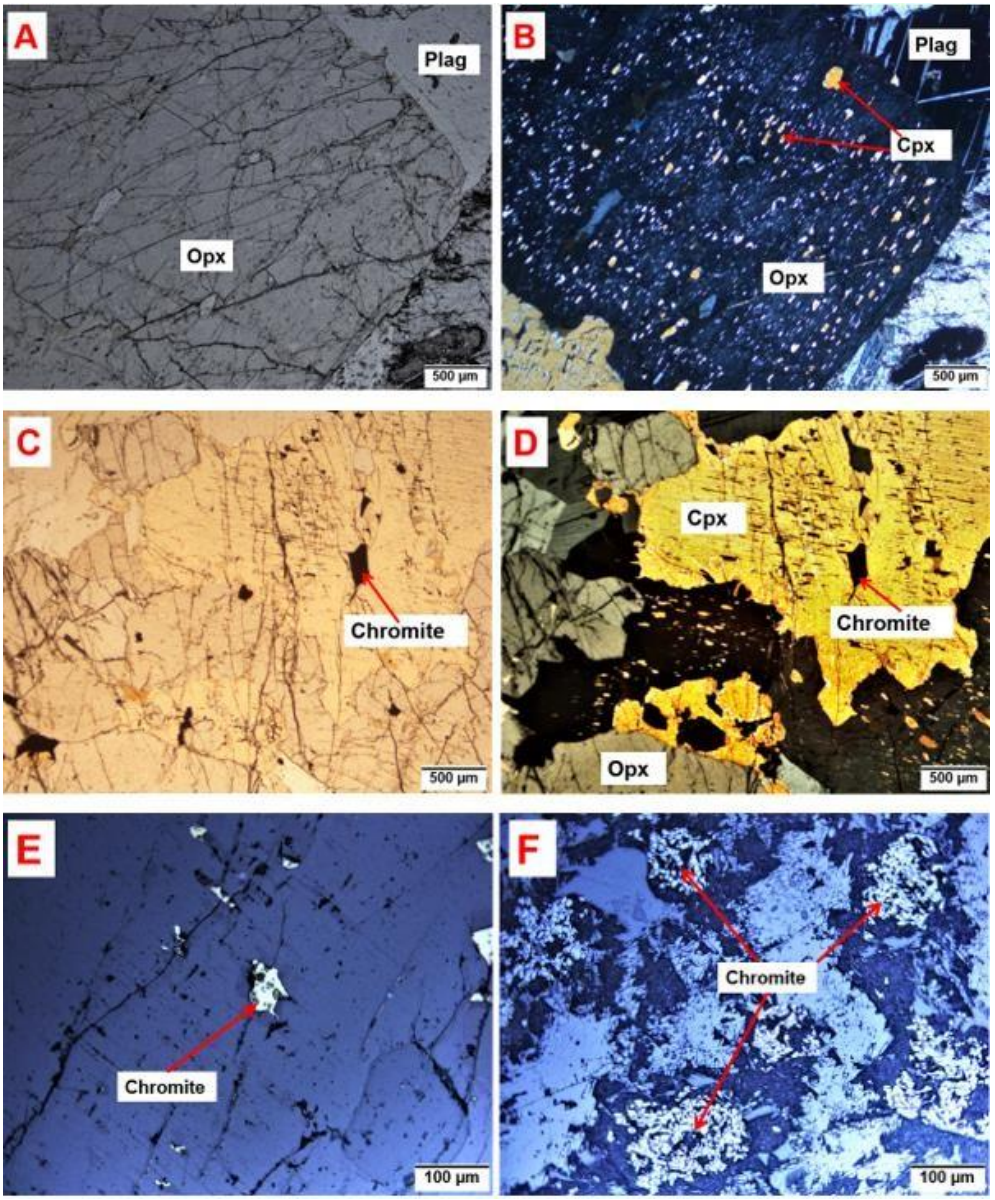


Figure 19*: Photomicrographs of Sample 5-10 5W-1 (A, B, C, and D) under 4x magnification PPL (plane polarised light) and XPL (crossed polarised light), and reflected light images (E and F) of chromite grains (20X). A) Euhedral orthopyroxene with interstitial plagioclase. B) Abundant clinopyroxene exsolution lamellae in orthopyroxene (same field of view as A). C) and D) Interstitial clinopyroxene with chromite inclusions. E) Chromite grain from C (slightly rotated) with some sulphides also present. F) The more dominant chromite grains with highly fractured surfaces.*

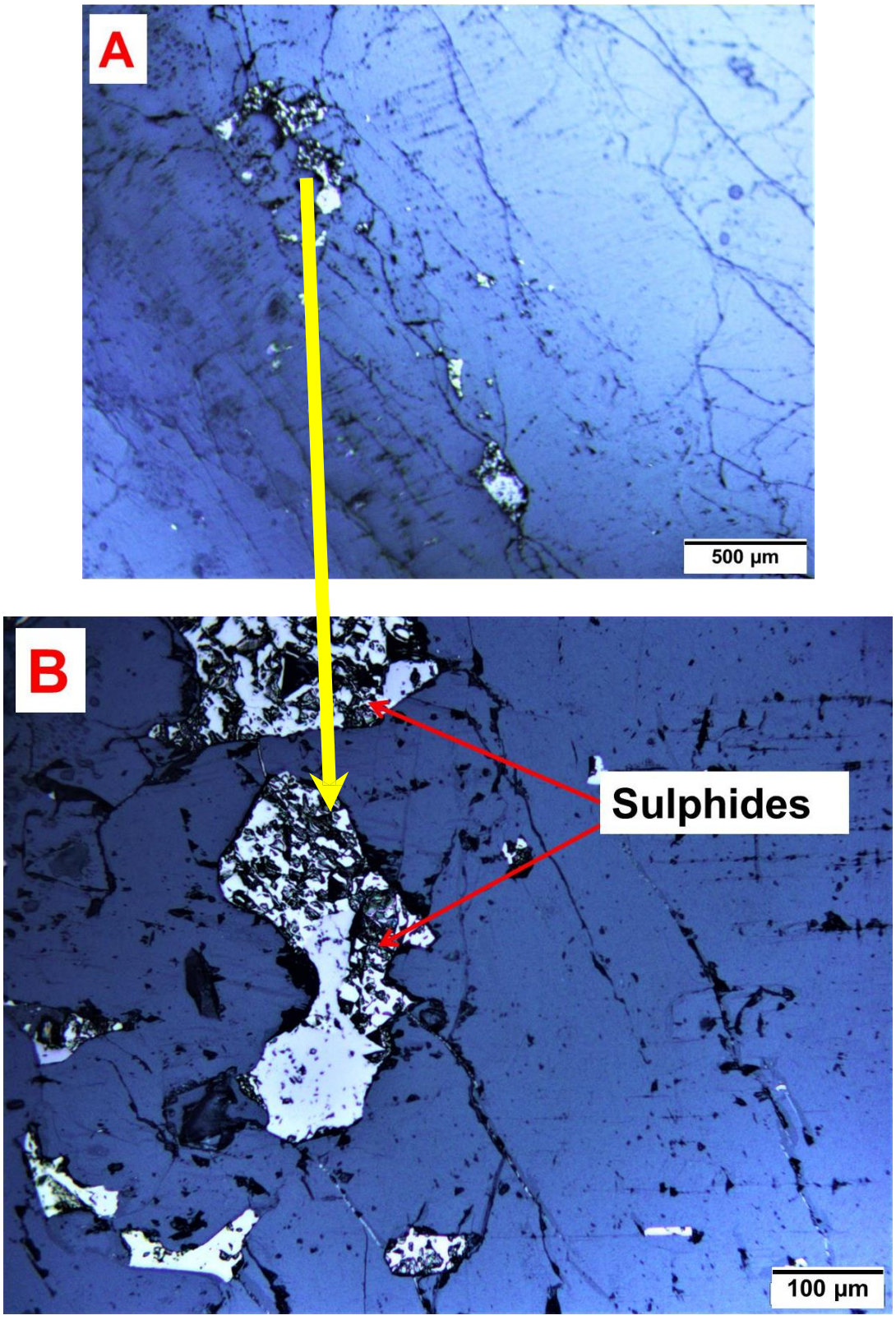


Figure 20: *Photomicrographs of Sample 5-10 5W-1 in reflected light. A) Chromite with interstitial sulphides along a fractured zone. B) A close-up of the sulphides along the fractured plane (20x magnification, reflected light).*

7.2.3. Sample 5-10 5W-2

Sample 5-10 5W-2 is medium-grained, consisting of two types of lithologies. The top half of the sample consists of approximately 70% plagioclase, 20% orthopyroxene and 10% clinopyroxene. Plagioclase in the top half of the sample is a cumulus phase, with interstitial orthopyroxene forming subhedral and anhedral grains (Fig. 21A-D). The bottom half of the sample consists of approximately 70% orthopyroxene, 25% plagioclase and 5% clinopyroxene. Orthopyroxene occurs as a coarse-grained cumulus phase surrounded by interstitial plagioclase. Minor clinopyroxene exsolution lamellae within the orthopyroxene is present (Fig. 21D). There are inclusions of euhedral and anhedral chromite within the larger orthopyroxene grains in the bottom half of the sample (Fig. 21E & F), albeit in smaller quantities compared to sample 5-10 5W-1.

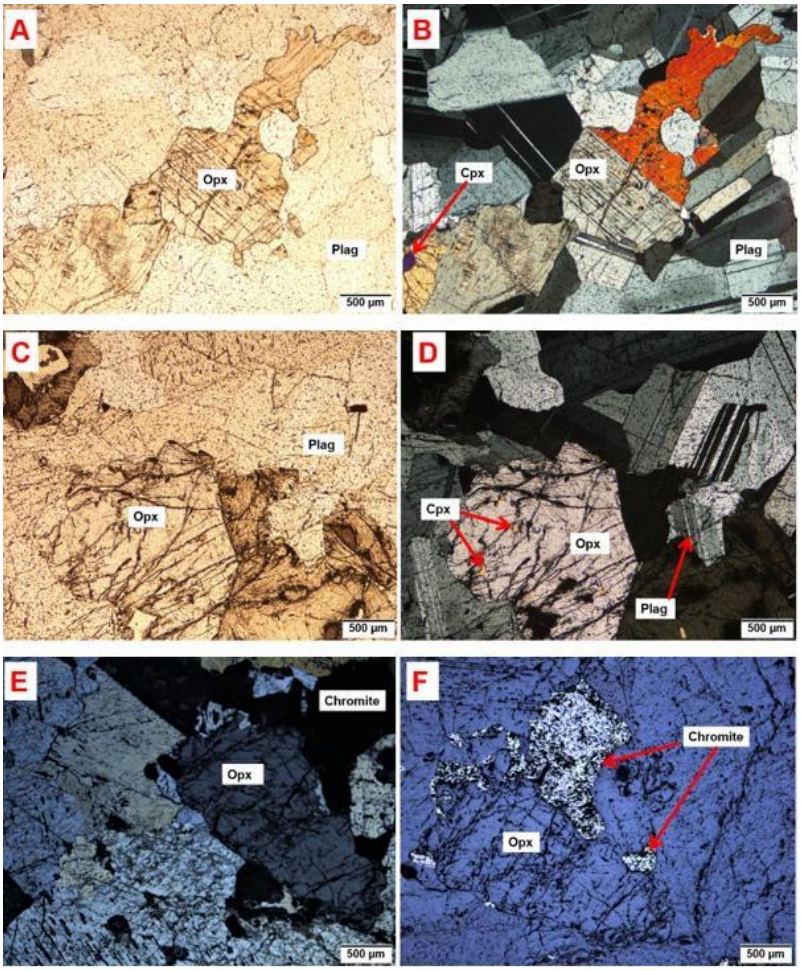


Figure 21: Photomicrographs of sample 5-10 5W-2 (A, B, C, D, E, F) under 4x magnification PPL (plane polarised light) and XPL (crossed polarised light). A) & B) Cumulus plagioclase with interstitial orthopyroxene and minor clinopyroxene. C) & D) Photomicrographs with minor clinopyroxene exsolution in orthopyroxene. E) Chromite within the orthopyroxene-dominant matrix at the bottom half of the sample. F) Chromite in reflected light.

7.2.4. Sample 9-10 4W

Sample 9-10 4W is medium-grained and texturally heterogeneous with plagioclase-rich enclaves. There is noticeable grading from norite into leuconorite with orthopyroxene enclaves, which are approximately 1 cm long. It consists of 50% plagioclase, 45% orthopyroxene and 5% clinopyroxene. The plagioclase is cumulus with anhedral, interstitial orthopyroxene and the minor interstitial clinopyroxene forming discontinuous rims at the edge of the orthopyroxene with minor exsolution lamellae into the orthopyroxene. There are trace amounts of sulphide, approximately 1 to 2 mm in size.

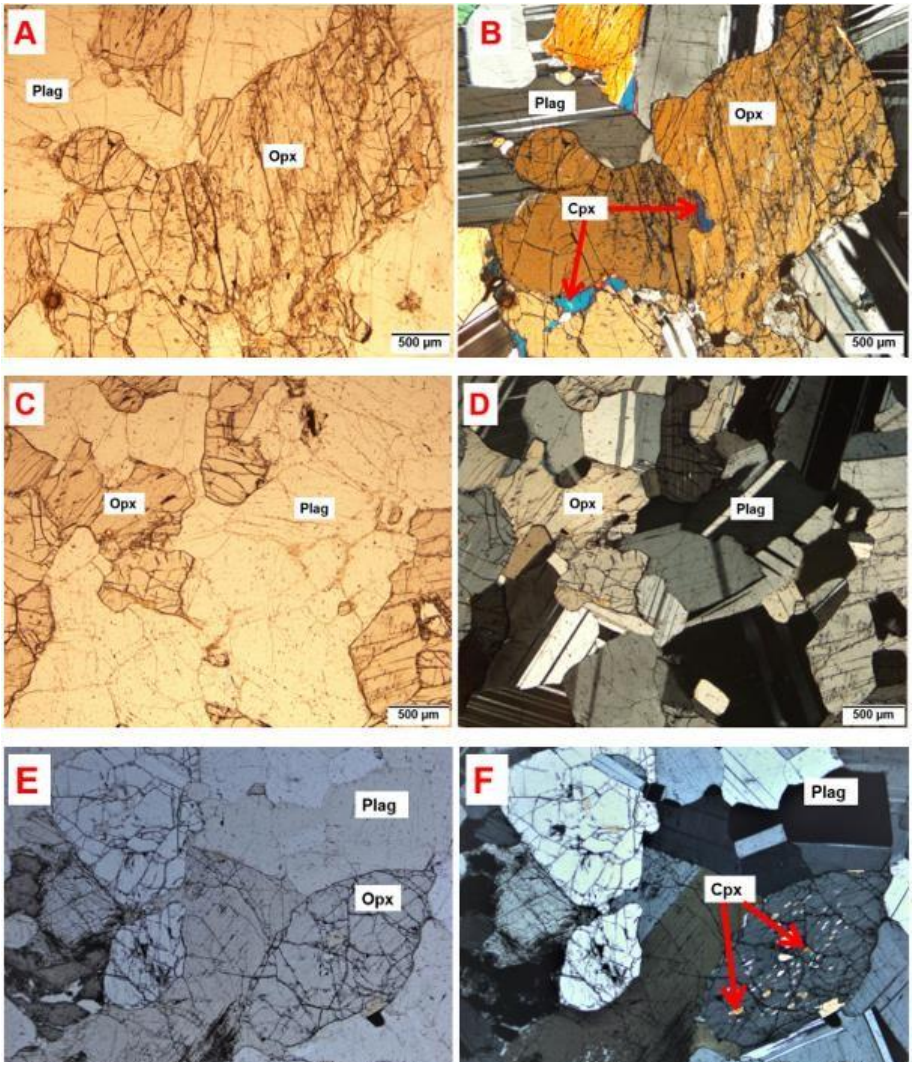


Figure 22*: Photomicrographs of sample 9-10 4W depicting the main petrographic features under 4x magnification PPL (plane polarised light) and XPL (crossed polarised light). A) & B) Noritic phase of the sample with plagioclase, orthopyroxene and minor clinopyroxene with discontinuous rims around the orthopyroxene. C) & D) The leuconorite phase of the sample with dominant cumulus plagioclase and interstitial orthopyroxene. E) & F) Exsolution lamellae of clinopyroxene in orthopyroxene.*

7.2.5. Sample HW

Sample HW is medium-grained and texturally homogenous and is part of the Merensky Cyclic Unit (MCU). It displays an adcumulate texture, rich in orthopyroxene and plagioclase. It consists of 50% orthopyroxene, 45% plagioclase and 5% clinopyroxene. The more dominant orthopyroxene is typically subhedral/anhedral and medium to coarse-grained. Plagioclase is mostly interstitial with euhedral laths that occur as inclusions in the orthopyroxene grains (Fig. 23B). The less dominant clinopyroxene is also interstitial with exsolution lamellae within the orthopyroxene and some forming discontinuous rims around the plagioclase (Fig. 23B). There are trace amounts of sulphide approximately 1 mm to 2 mm in size.

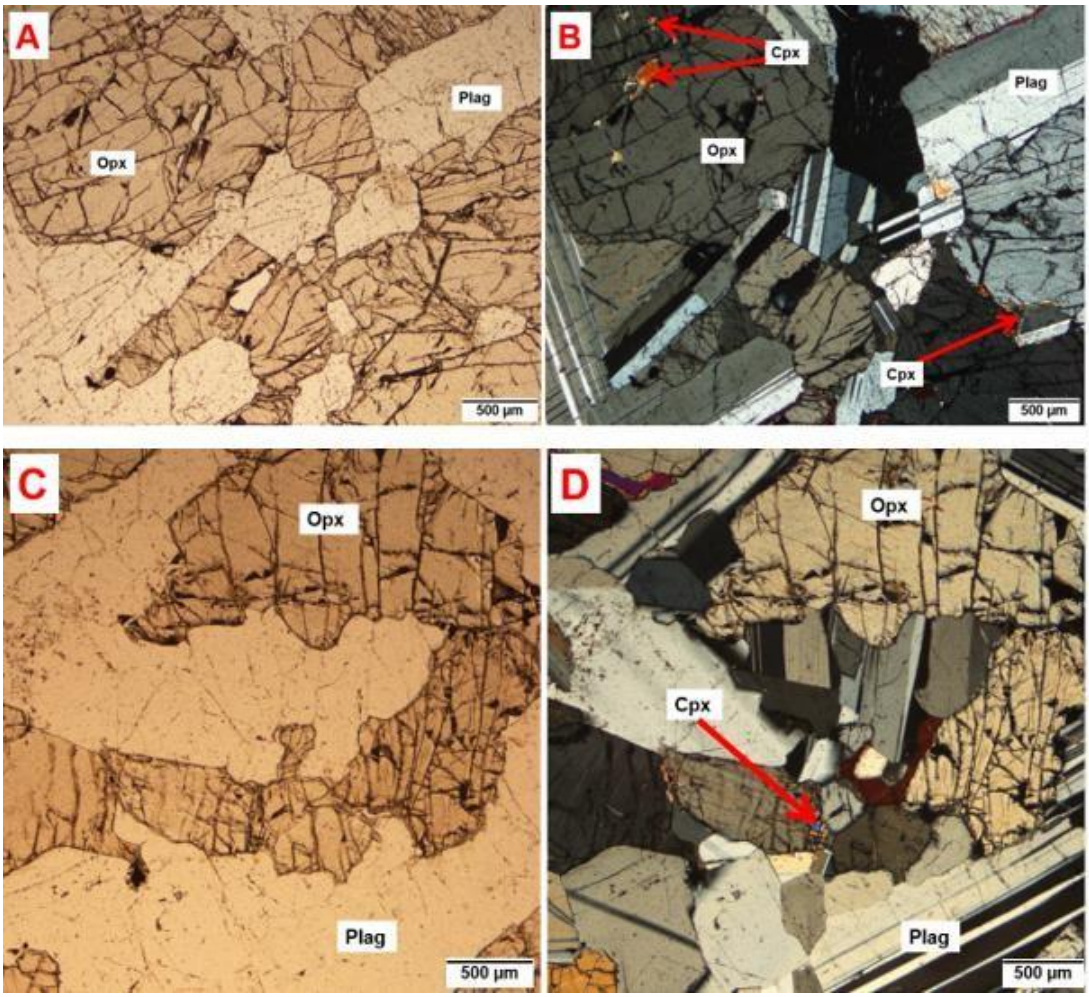


Figure 23: Photomicrographs of sample HW depicting the main petrographic features under 4x magnification PPL and XPL. A) Anhedral orthopyroxene with interstitial plagioclase. B) Clinopyroxene with minor exsolution lamellae as well as discontinuous rims around plagioclase. C) & D) Subhedral orthopyroxene with interstitial plagioclase and clinopyroxene.

7.3. Whole rock geochemistry

7.3.1. Major Elements

The major element data has not been obtained from the Earth Observatory at the University of the Witwatersrand due to a breakdown of the X-ray fluorescence (XRF) equipment. Therefore, no major element results will be presented here.

7.3.2. Trace Elements

Sample 5-10 5W-1, which is part of the Merensky Reef, is enriched in Heavy Rare Earth Elements (HREE) relative to Light Rare Earth Elements (LREE), while the other four samples are enriched in LREE relative to HREE (Fig. 24). Pronounced negative Th and Nb anomalies are noted in all samples except for sample 5-10 5W-1, which shows a positive Nb anomaly.

Sample FW has the lowest concentrations of compatible elements, such as Ni, Cr, Cu and V, with the highest concentration of Sr as well as elevated Eu concentrations. This is attributed to its high plagioclase content, with Sr and Eu favouring plagioclase. This sample also has a high Ce/Yb ratio and the lowest Ti content (Fig. 26). When compared to the other samples, Sample FW has the lowest REE concentrations (Fig. 25).

Sample 5-10 5W-1 has the highest concentrations of most trace elements amongst the samples (Fig. 24), except for Ba, La, Sr and Eu, which are compatible with plagioclase (Wilson & Chunnett, 2006). Relatively greater quantities of Ni, Cr, Cu, Co and Zn (Table 1) are attributed to the sample being orthopyroxene-rich with some chromite and sulphide. This sample exhibits low Ce/Yb ratios (Fig. 26), consistent with its high orthopyroxene content. Sample 5-10 5W-1 has Zr concentrations that are almost double those of Sample FW, 9-10 4W, and 5-10 5W-2, and 23% higher than Sample HW, which is also orthopyroxene-dominant.

Sample 5-10 5W-2 and 9-10 4W are similar in that they both have concentrations of Ni, Cr, Cu, Co and V that are significantly lower compared with sample 5-10 5W-1. Both samples have significantly elevated Eu concentrations. Sample 5-10 5W-2 also has the lowest Zr concentrations, and sample 9-10 4W has a Cu concentration that is 80% lower than that of sample 5-10 5W-2. When compared to other samples, sample 9-10 4W has relatively low Ce/Yb ratios with a slightly high Ti concentration, while sample 5-10 5W-2 has an intermediate Ce/Yb ratio as well as an intermediate Ti concentration (Fig. 26). This is attributed to the samples having an abundance of both plagioclase and orthopyroxene, rather than being

dominant in one of these two minerals. These samples have the lowest content of incompatible trace elements such as Th, U, Nb and Zr.

Sample HW has relatively high concentrations of Cr and significantly lower concentrations of Ni, Cu, Co, and V. The sample is also enriched in LREE/HREE with an Eu concentration that is 35% higher than that of 5-10 5W-1 (Fig. 25). This is attributed to the sample being rich in both orthopyroxene and plagioclase, but with orthopyroxene being more dominant. Sample HW has relatively low Ce/Yb ratios, with a relatively low Ti concentration (Fig.26).

Trace Element Analysis					
	FW (ppm)	**HW (ppm)**	**9-10-4W (ppm)**	**5-10-5W-1 (ppm)**	**5-10-5W-2 (ppm)**
Li	3.4	4.0	4.7	2.8	3.9
P	26.7	26.3	23.6	25.7	26.1
Sc	7.8	14.6	20.8	27.0	13.3
Ti	478.5	887.7	1099.9	1773.4	1014.9
V	52.6	81.2	138.8	187.1	90.1
Cr	826.9	1769.9	803.2	2640.4	834.9
Co	30.1	58.5	37.3	147.7	46.0
Ni	173.3	494.9	223.3	3558.1	318.5
Cu	4.0	99.4	22.8	1912.6	115.2
Zn	26.8	53.5	39.4	103.9	48.4
Ga	15.8	10.9	15.5	5.9	14.6
AS	0.1	0.1	0.1	0.2	0.1
Rb	0.8	1.4	0.5	1.0	0.5
Sr	392.5	231.0	322.3	58.7	279.6
Y	1.0	2.5	4.3	6.3	2.8
Zr	3.6	4.6	3.5	6.4	2.2
Nb	0.2	0.1	0.0	4.3	0.4
Sn	0.2	0.3	0.1	0.3	1.1
Sb	0.0	0.0	0.0	0.0	0.0
Cs	0.0	0.1	0.0	0.0	0.0
Ba	47.7	42.5	37.2	15.1	54.0
La	1.4	1.7	1.7	1.1	2.7
Ce	2.8	3.3	3.6	2.9	5.0
Pr	0.3	0.3	0.5	0.4	0.5
Nd	1.0	1.3	2.2	2.0	2.0
Sm	0.2	0.3	0.6	0.6	0.4
Eu	0.3	0.2	0.5	0.2	0.5
Gd	0.2	0.3	0.7	0.7	0.4
Tb	0.0	0.1	0.1	0.1	0.1
Dy	0.2	0.4	0.7	1.0	0.4
Ho	0.0	0.1	0.1	0.2	0.1
Er	0.1	0.3	0.4	0.7	0.3
Tm	0.0	0.0	0.1	0.1	0.0
Yb	0.1	0.3	0.4	0.8	0.4
Lu	0.0	0.1	0.1	0.1	0.1
Hf	0.1	0.1	0.1	0.2	0.1
Ta	1.1	0.0	0.0	0.4	0.1
W	0.2	0.2	0.2	5.6	0.4
Tl	0.0	0.0	0.0	0.0	0.0
Pb	0.7	1.7	0.7	9.0	1.9
Th	0.1	0.1	0.0	0.1	0.0
U	0.0	0.0	0.0	0.0	0.0

Table 1*: Trace element concentration data for the five samples analysed in this study.*

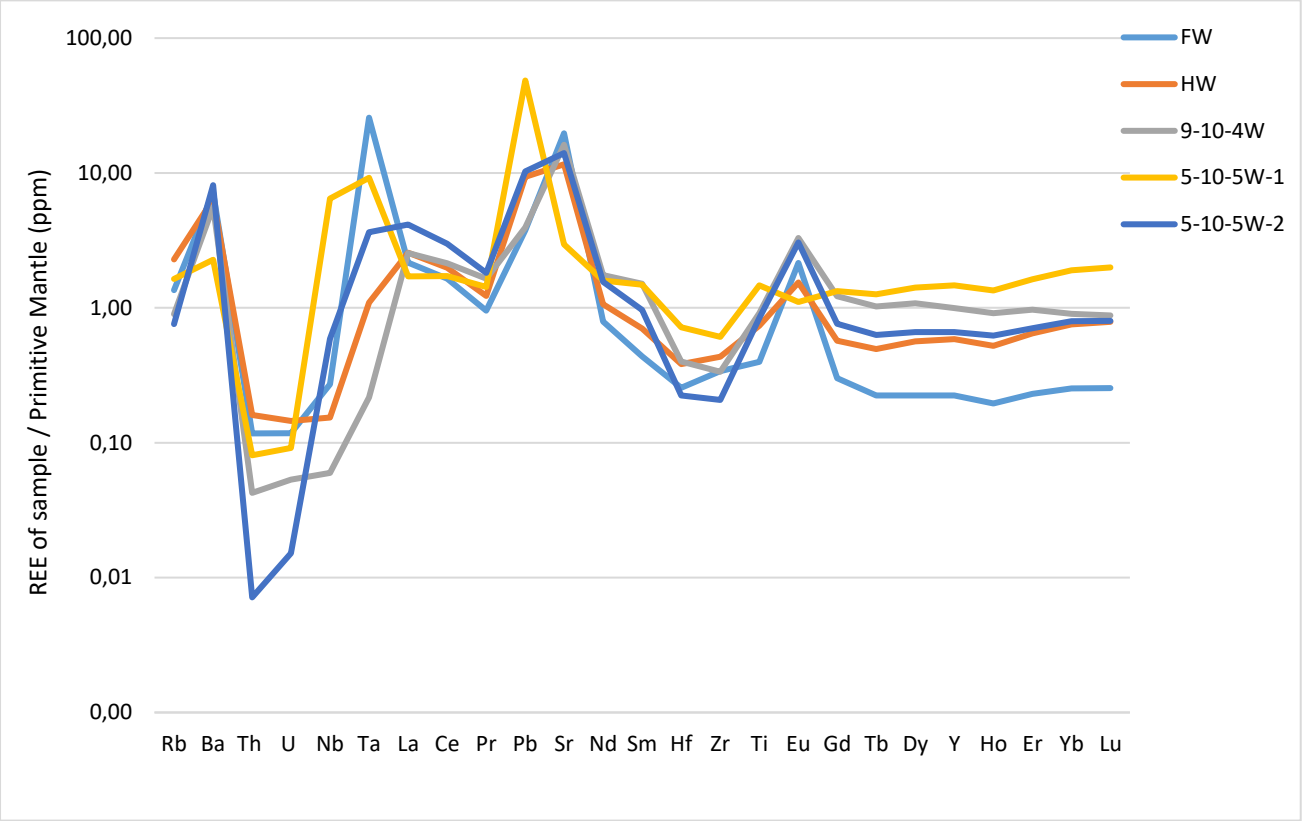


Figure 24*: A graph representing the Primitive Mantle normalised patterns for the samples in the study. Note that sample 5-10 5W-1 has higher concentrations of trace elements compared to the other samples, except for Ba, La, Sr and Eu.*

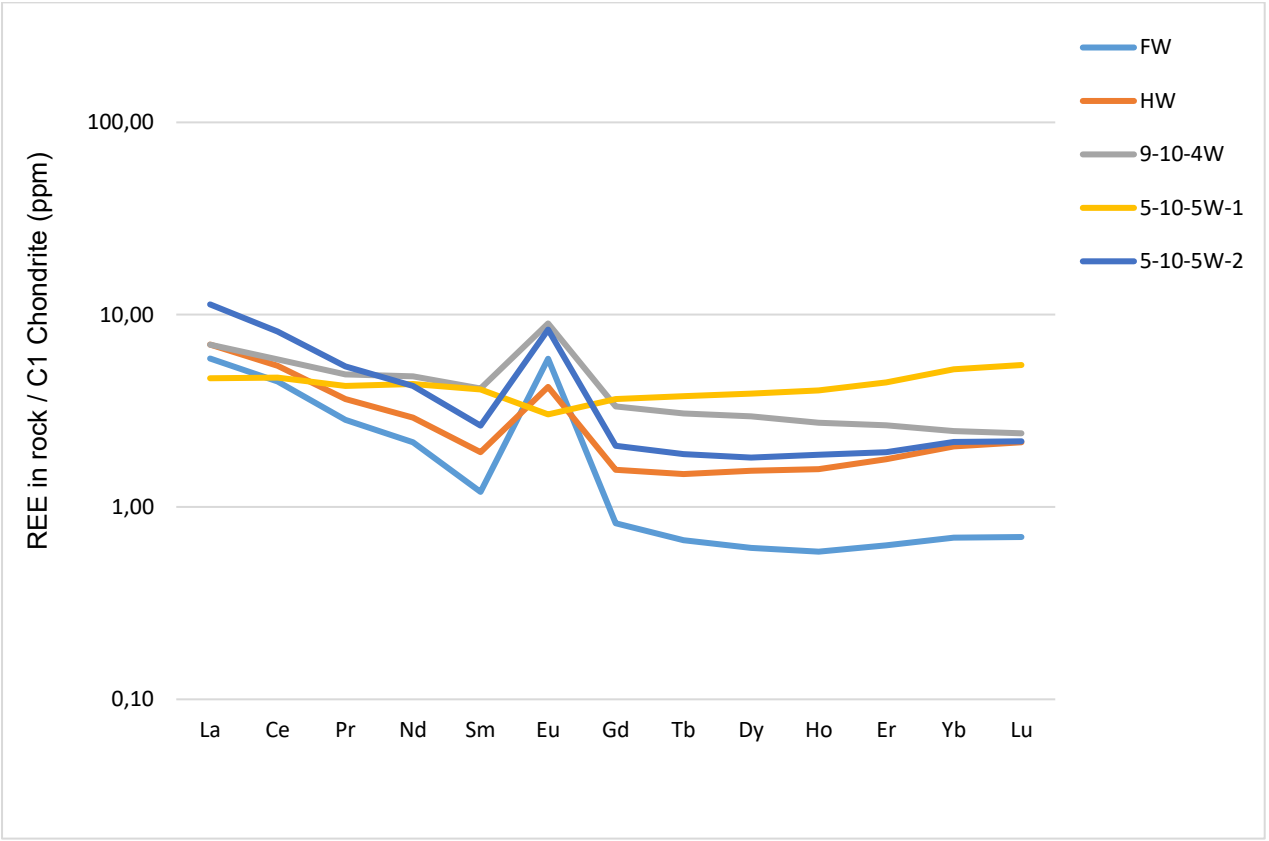


Figure 25: A graph representing chondrite-normalised REE patterns for the samples analysed in this study. Note that sample 5-10 5W-1 has a distinctively flatter profile and a minor negative Eu anomaly compared to the other samples

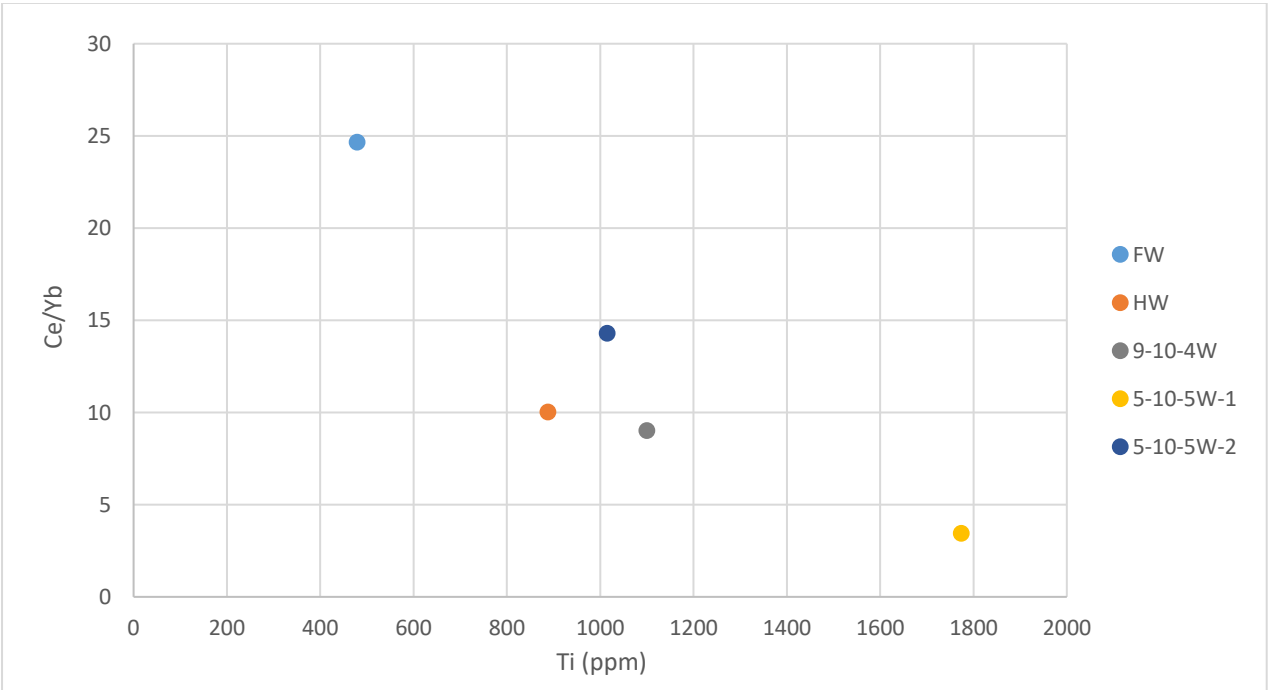


Figure 26*: A scatter plot of Ce/Yb versus Ti (ppm). The Ce/Yb ratio represents the enrichment of LREE relative to HREE.*

7.4. Grade analysis

The planned 4E (Pt, Pd, Rh & Au) face grade for P2 Reef was 8.63 g/t and 7.05 g/t at shaft-1 (Table 3) and shaft-2 (Table 5), respectively. The assayed face grades, however, indicate lower values for both shaft-1 and shaft-2. Additionally, laboratory results of the norite bodies intersected on both stopes are 0 g/t, confirming that these bodies are barren in terms of 4E content.

The face grade from shaft-1 stope decreased by 1.36 g/t to an assayed value of 7.27 g/t for the reef. There was a further decrease of 5.02 g/t for the stope with the addition of the barren norite resulting in a grade of 2.25 g/t (Fig. 27). The face grade from shaft-2 stope decreased by 0.39 g/t to an assayed value of 6.66 g/t for the reef, with a further decrease of 4.53 g/t for the stope when dilution caused by the barren norite body is considered. This resulted in a stope grade of 2.13 g/t (Fig. 28).

Reef			Norite body		
Grade (g/t)	**Volume (m^3)**	**Density (g/m^3)**	**Grade (g/t)**	**Volume (m^3)**	**Density (g/m^3)**
7.27	1.20	3.41	0.00	2.76	3.30

Table 2*: Assayed values for the reef and norite body at shaft-1.*

Planned face grade (g/t)	Grade drop (g/t)	Assayed face grade (g/t)	Norite Dilution (g/t)	Final face grade (g/t)	Grade dilution (%)
8,63	1,36	7,27	5,02	2,25	69,03

Table 3*: Shaft-1 stope planned face grade and the assayed face grade. Note that the dilution caused by the barren norite body has affected the final face grade, reducing it from an initial assayed value of 7.27 g/t to 2.25 g/t. This equates to a 69% dilution.*

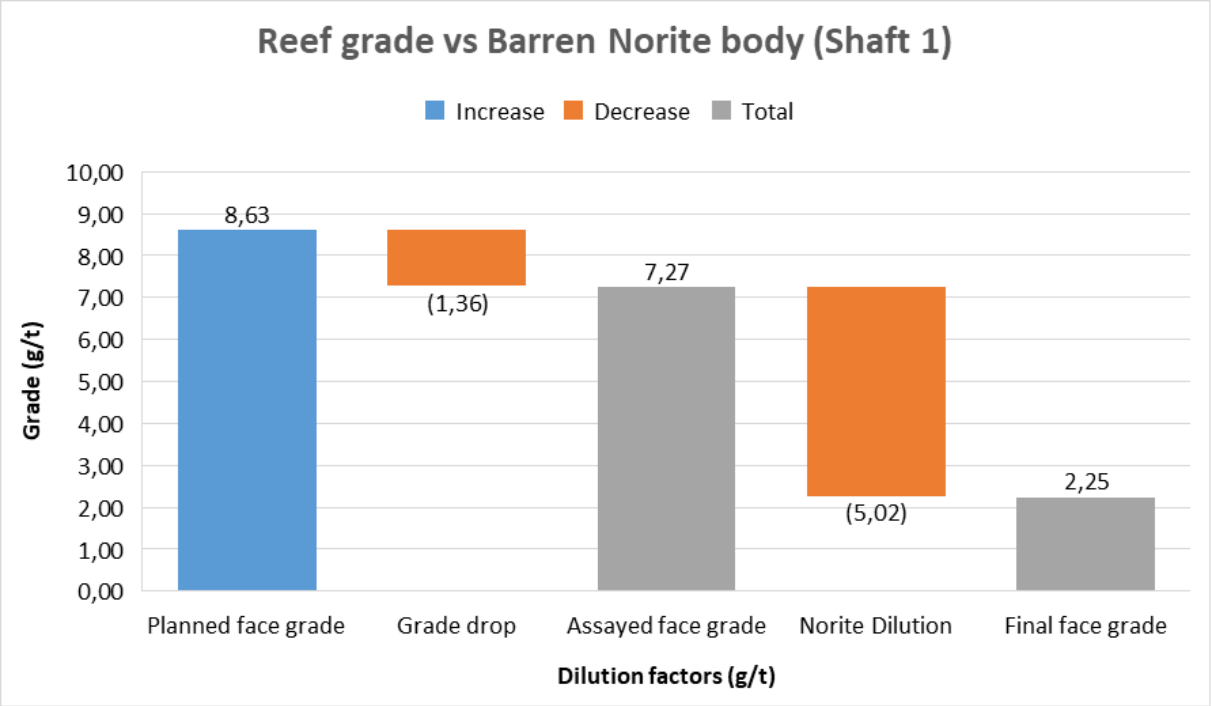


Figure 27*: A waterfall chart representing how the dilution from the norite body affected the face grade at shaft-1. The face grade decreases significantly to 2.25 g/t from a planned grade of 8.63 g/t. The major contributor is the dilution caused by the grade of the norite body at 5.02 g/t from the assayed grade of 7.27 g/t.*

REEF			NORITE BODY		
Grade (g/t)	**Volume (m^3)**	**Density (g/m^3)**	**Grade (g/t)**	**Volume (m^3)**	**Density (g/m^3)**
6.66	1.20	3.41	0.09	2.76	3.30

Table 4*: Assayed values for the reef and norite body at shaft-2*

Planned face grade (g/t)	**Grade drop (g/t)**	**Assayed face grade (g/t)**	**Norite Dilution (g/t)**	**Final face grade (g/t)**	**Grade dilution (%)**
7.05	0.39	6.66	4.53	2.13	68.05

Table 5: Shaft-1 stope planned face grade and the assayed face grade. Note that the dilution caused by the barren norite body has affected the final face grade, reducing it from an initial assayed value of 6.66 g/t to 2.13 g/t. This equates to a 68% dilution.

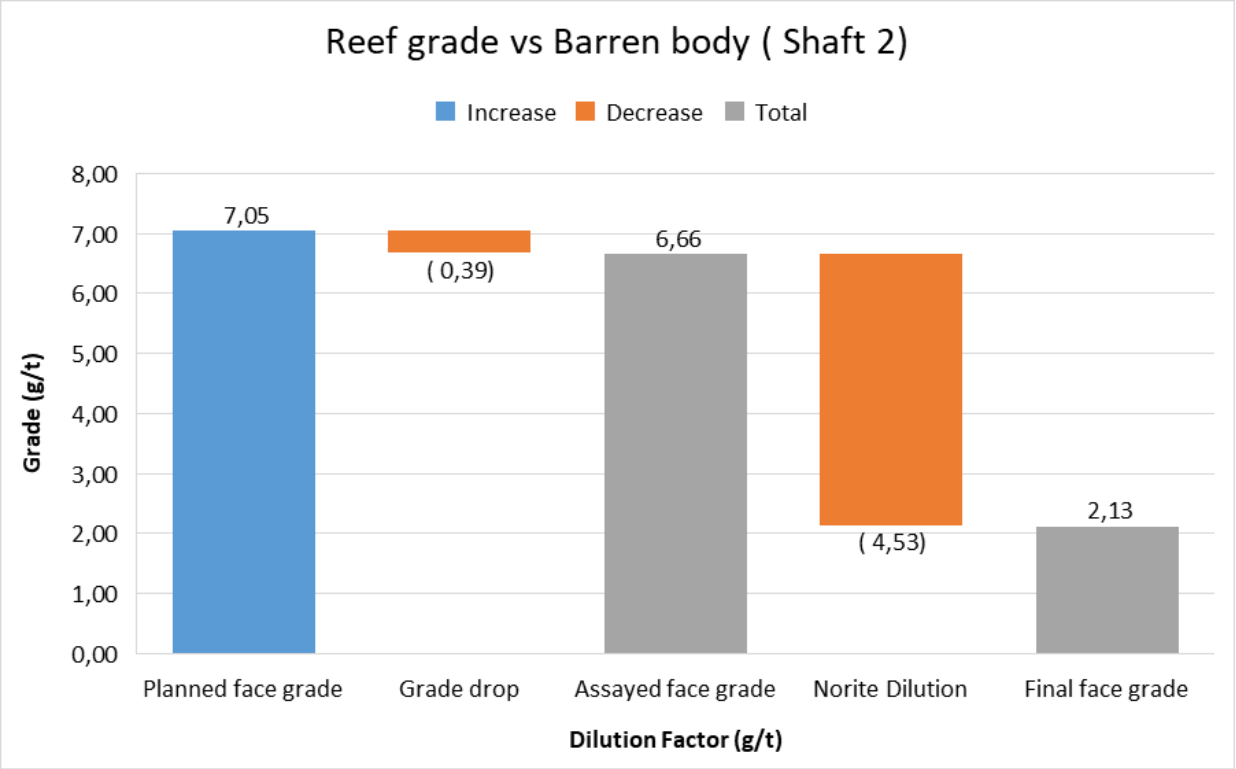


Figure 28*: A waterfall chart representing how the dilution from the norite body affected the face grade at shaft-2. The face grade decreases significantly to 2.13 g/t from a planned grade of 7.05 g/t. The major contributor is the dilution caused by the norite body at 4.53 g/t from an assayed grade of 6.66 g/t.*

8. DISCUSSION

Numerous studies have been conducted on the Merensky Reef in the Western Limb of the Bushveld Complex, with some studies mainly focused on the origin of the Regional Potholed Reef (RPR). Potholes have been described as local layering disturbances and irregularities that form transgressive contacts of the reef in relation to their footwall (Viljoen, 1999; Smith & Basson, 2005, 2006; Maier et al., 2012; Latypov et al., 2017a; Hunt et al., 2018). This study is focused on the RPR at the south-western extension of Zondereinde Mine (Northam Platinum), where norite and anorthosite bodies truncate the stratigraphy on the P2/FWP2 Reef horizon. This study aimed to examine and understand the nature and impact of these norite-anorthosite bodies within the reef by constraining their effect on mining and PGE grade. The objectives included determining how these norite-anorthosite bodies fit into the magmatic stratigraphy, documenting their size variations, and contact relationships with the host rocks. Another objective of this study was to establish whether there is an association between the norite-anorthosite bodies and the Iron Rich Ultramafic Pegmatoids (IRUP), as well as to investigate their relationship to potholes.

Norite bodies from underground stopes have been analysed by petrography and trace element geochemistry to compare them to similar-looking norites in the hanging wall and the footwall of the Merensky Cyclic Unit. Mitchell et al. (2019) noted that in the Amandelbult enclave, the UG-2 hanging wall pyroxenite and the Pseudoreef above it contain thin norite and/or anorthosite units, with the harzburgite of the Pseudoreef appearing to be intercalated with these norite and/or anorthosite units. Although these authors noted these units, there is no detailed information regarding their nature or how they affect the magmatic stratigraphy. Furthermore, there has been no investigation regarding these bodies in the Merensky Reef. This could either be because they have not been intersected in other mines, or they have been overlooked and regarded as insignificant.

In the UG-2 Reef, however, Latypov et al. (2017b) noted that leuconorite and anorthosite can invade the hanging wall pyroxenite and cut through the UG-2 as well as the underlying UG-1 chromitite. This has also been investigated by Maier et al. (2016) at Smokey Hills mine in the Eastern Bushveld Complex, where transgressive and irregular anorthosite in the UG-2 and UG-3 chromitites have been observed. In their study, Maier et al. (2016) proposed that the anorthosite potholes formed by the late-stage solidification of anorthosite mushes within the cumulate pile (Fig. 29). They suggested that the transgressive anorthosite was structurally controlled, with changes in the shape of the potholes resulting from magma eroding the side walls. The process has been summarised in Figure 29 below.

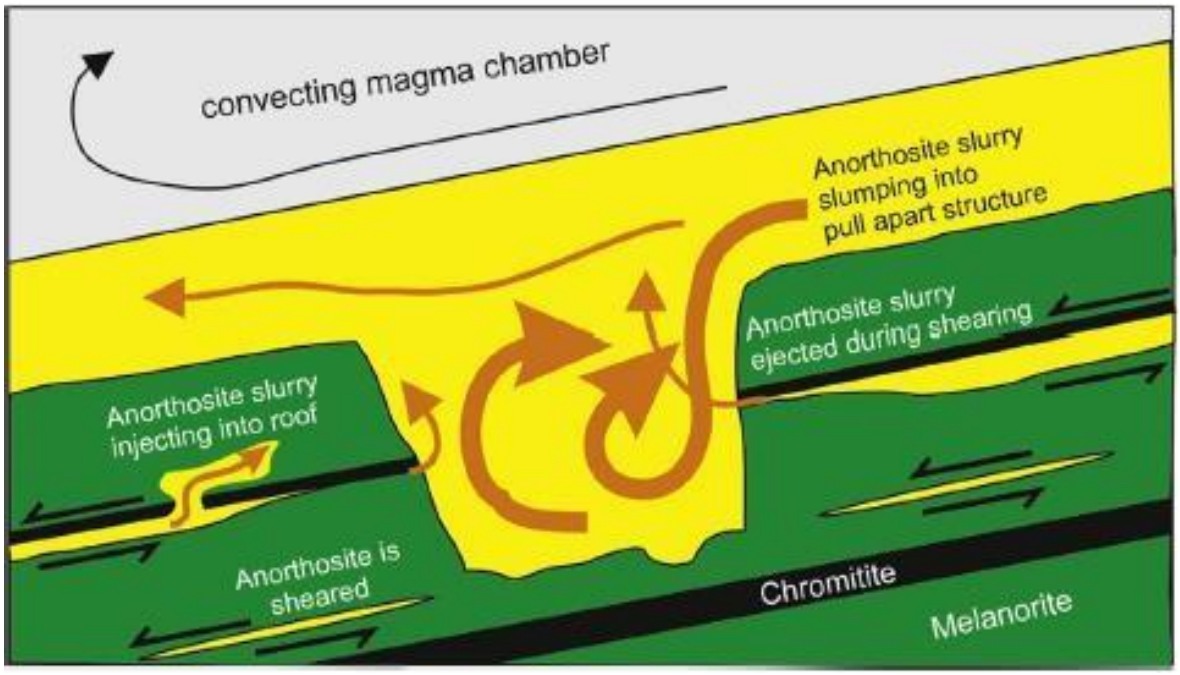


Figure 29*: A diagram by Maier et al. (2016) illustrating how the anorthosite pothole at Smokey Hills formed.*

Potholes, which are transgressive features in the Bushveld Complex, have been interpreted to have formed from thermochemical erosion of cumulates from a batch of hot, dense, primitive magma that replenished the evolving magma chamber (Maier et al, 2012; Latypov et al., 2015).

According to Maier et al. (2016), the formation of igneous layering in the Bushveld Complex and other mafic-ultramafic intrusions results from subsidence and the sorting of noritic proto-cumulate through a combination of magmatic and structural processes. They propose that at Smokey Hills in the Eastern Bushveld, a large amount of plagioclase-rich layers remained unsolidified for long periods due to buoyant residual liquid. The unsolidified plagioclase would later serve as lubrication planes, promoting structural failure and pull-apart structures that may form during this process when the cumulate layers bend due to ground settling. These extensional structures, especially in regions experiencing more stretching, create openings for the injection of anorthosite slurries from the buried anorthosite mushes that were remobilised because of hot shearing within the cumulate pile, into the partially solidified cumulate layers, leading to the formation of large anorthosite potholes (Fig. 29).

8.1. Integrating textures, mineralogy, and trace element geochemistry

Petrographic analysis reveals distinct mineralogical compositions and textures across all samples in this study, with trace element analysis providing further insight into the geochemical differentiation and magmatic processes of the rock types. Maier et al. (2012) have explained

that parental magma characteristics, mineral proportions, trapped melt composition, and late-stage fluid activity are factors that partly influence the distribution of incompatible trace elements in the cumulate rocks. Some of these processes are considered in the interpretations below.

The norites at Zondereinde Mine are medium to coarse-grained, with some transitioning into leuconorite, due to their increased plagioclase content. There is a poikilitic texture with orthopyroxene oikocrysts enclosing plagioclase chadacrysts and the margins of the orthopyroxene intergrown into the plagioclase laths (e.g., Figures 18A and 23A). Poikilitic textures indicate that new magma was injected and mixed with pre-existing resident magma in the chamber, entrapping the preceding plagioclase grains, which resulted in the intercumulus texture as well as the formation of oikocrysts (Mitchell et al., 1998; Prevec et al., 2005; Beukes et al., 2016).

All samples contain interstitial clinopyroxene which occasionally appears as exsolution lamellae in orthopyroxene grains (e.g., Fig. 19B, 21D, 22F and 23B) as well as discontinuous rims around plagioclase grains (Fig. 18B and 23B) and orthopyroxene grains (Fig. 21D). Beukes et al. (2016) have attributed exsolved lamellae to a recrystallisation process and suggest that clinopyroxene rims are because of the exsolution of clinopyroxene-compatible elements migrating towards the boundaries of the orthopyroxene and/or plagioclase during cooling.

Trace element observations from the samples in this study indicate a close relationship to trace element observations by Arndt et al. (2005) as well as Wilson & Chunnett (2006), who noted that there is a difference between pyroxenite and norite when compared using REE. Wilson & Chunnett (2006) concluded that rock types which are plagioclase-dominant show a positive Eu anomaly as opposed to orthopyroxene-rich rock types. This is evident in Figure 25 with sample 5-10 5W-1, an orthopyroxenite, which displays a negative Eu anomaly compared to the norite samples.

The Pseudoreef orthopyroxenite (sample 5-10 5W-1) is orthopyroxene-dominant with interstitial plagioclase and clinopyroxene. The negative Eu anomaly in the sample indicates a less favourable environment for Eu retention (i.e., less plagioclase). The sample has relatively high concentrations of compatible elements, such as Ni, Cr, and Cu, which is consistent with its orthopyroxene-rich composition and the presence of sulphide and chromite. The sample also displays positive Nb, Ta, Zr, and Hf anomalies (Fig. 24). These High Field Strength Elements (HFSE) are associated with high temperatures and partial melting and become compatible with orthopyroxene in these conditions (Nikitina et al., 2016). This is also consistent with the observations of Maier et al. (2012), who noted higher concentrations of incompatible trace elements in ultramafic rocks when compared to feldspar-rich rocks. This is because

ultramafic rocks have relatively higher trapped liquid components. Maier et al. (2012) also note that Zr contents between 5 and 20 ppm are proportional to 5–30% trapped melt content. Sample 5-10 5W-1 has a Zr content of 6.4 ppm, which is the highest amongst the samples in this study. This indicates that the sample may contain late-stage residual melt that got trapped during solidification.

Sample FW shows a predominance of plagioclase with interstitial orthopyroxene and clinopyroxene. This adcumulate texture indicates a plagioclase-dominated crystallisation environment. It also exhibits enrichment in LREE/HREE (Fig. 25) and shows pronounced negative anomalies for elements such as Th and Nb (Fig. 24), suggesting a plagioclase-rich source, derived from a melt with much lower incompatible trace elements and higher concentrations of Sr and Eu. Such features are characteristic of norites.

Sample HW displays an adcumulate texture. Roberts et al. (2006) noted that trace amounts of sulphides are present in the norite of the MCU, which was also observed in Sample HW. This sample has an Eu concentration of 1.54 ppm, which is the lowest of the four noritic samples. This is due to its more melanoritic nature, with the sample being orthopyroxene dominant. This is also consistent with the conclusion by Wilson & Chunnett (2006).

Samples 5-10 5W-2 and 9-10 4W, which represent the norite bodies on the reef horizon, have been noted to comprise transitional lithologies between norite and leuconorite with varying proportions of plagioclase, orthopyroxene and clinopyroxene. Similar to Sample FW, these samples were formed from a liquid with high concentrations of Eu and Sr but display trace elements that are intermediate between Sample FW and Sample HW.

Strontium, a trace element more compatible with plagioclase, shows positive anomalies for all the norite samples (Fig. 24). This is also evident in the high Sr values (Table 1). However, incompatible trace elements are lower in the norite samples when compared to Sample 5-10 5W-1, which is an orthopyroxenite. This is because norite is formed from a liquid with lower incompatible trace element concentrations when compared to the liquid that formed pyroxenite (Arndt et al., 2005). Sample HW has the lowest concentration of Sr among the norites, while Sample FW, a plagioclase-rich leuconorite, has the highest Sr value.

The hanging wall norite (Samples HW) and the norite bodies (Samples 9-10-4W and 5-10 5W-2) show similarities in their petrography and trace element data. Featuring medium-grained textures, these samples are both plagioclase- and orthopyroxene-dominant, with interstitial clinopyroxene often forming exsolution lamellae with orthopyroxene. Additionally, chromite and sulphide grains are present in these samples. These samples exhibit relatively low Ce/Yb ratios and intermediate Ti concentrations when compared to other samples, as shown in Figure 26. Their relatively higher Ti and Cr concentrations may be due to their proximity to the

Merensky Reef, thus resulting in these samples having trace amounts of sulphides. They are rich in Sr, Ba, and Ce concentrations, while Zn, Ni, Cu, and Pb concentrations are low. Sample 9-10 4W grades from norite into leuconorite, which is typical of the MCU, where the hanging wall norite grades into leuconorite and anorthosite. These similarities between the hanging wall norite and the norite bodies, in the study, indicate similar crystallisation processes and suggest that the norite bodies are part of the hanging wall stratigraphy.

The footwall “Streepies” norite (Sample FW), conversely, has the highest Ce/Yb ratio and the lowest Ti concentration when compared to the other noritic samples (Fig. 26). This is because of its high plagioclase content and the incompatibility of Ti with plagioclase. Furthermore, the sample displays a comparable Sr value to Sample 9-10 4W. This is attributed to Sample 9-10 4W grading from norite to leuconorite, due to its increasing plagioclase content.

Sample 5-10 5W-1 has high Ti concentrations, as visible in Figure 24, and its Nb and Pb concentrations are the highest indicating that the sample is part of the mineralised zone as confirmed by the presence of base metal sulphides and chromite (Fig. 20). Sample 5-10 5W-1 is the Pseudoreef orthopyroxenite directly below the Merensky Reef contact, which explains the presence of sulphides in this sample.

8.2. Origin of the norite and anorthosite bodies

The origin of anorthosite within layered intrusions remains unresolved (Maier et al., 2012); however, Cawthorn & Ashwal (2009) have discussed various hypotheses regarding anorthosite formation, suggesting it originates from the gravitational settling and sorting of plagioclase grains in the magma chamber. Their model suggests that plagioclase nucleates and crystallises in the magma chamber and is mechanically concentrated. They have also observed that most of the anorthosites in the Bushveld Complex are overlain by leucocratic rocks. Maier et al. (2012) proposed that anorthosites may be of an intrusive origin. In their study, they also argued that the intruding anorthosite magma at Smokey Hills Mine was a slurry containing an abundance of plagioclase crystals. Latypov et al. (2020) suggest that transgressive anorthosite as observed at Smokey Hill Mine formed from highly reactive superheated melts responding to lower pressure in the magma chamber, thereby replenishing the chamber as it evolves, and eroding the footwall cumulates before the plagioclase-saturated melt crystallised.

Field observations of the norite-anorthosite bodies in this study are consistent with potholing, with these bodies partially or completely replacing the hanging wall pyroxenite of the MCU above the Merensky Reef (Fig. 17B & D) and cutting through the layered reef stratigraphy (Fig. 17A & D). A sill-like intrusion of anorthosite with norite autoliths between the Merensky chromitite and hanging wall pyroxenite is also evident in Figure 17C. Underground mapping

and core logging have revealed the erratic distribution of these norite-anorthosite bodies and their variability in shape and size (Fig. 16).

The petrographic and trace element data collectively reveal the complex magmatic history and differentiation processes that have shaped the norite bodies in this study. The variations in trace element patterns and petrographic characteristics across the samples suggest a dynamic magmatic environment with multiple phases of intrusion and crystallisation. The plagioclase-rich norites and anorthosites exhibit distinct LREE/HREE-enrichment, indicative of their crystallisation environment and magmatic differentiation. Norite is less enriched in incompatible trace elements with greater enrichment of Sr and Eu, as noted in the study by Arndt et al. (2005), and demonstrated in Figure 24. The sampled norite bodies (Samples 9-10 4W and 5-10 5W-2) indicate similar crystallisation processes and have petrographic and geochemical similarities with the hanging wall norite (Sample HW). It is suggested that these norite-anorthosite bodies formed from the same magma sources with late-stage solidification of anorthosite mushes (Maier et al., 2016). The mechanism of crystal settling and sorting, as suggested by Cawthorn & Ashwal (2009), also applies. They suggest that before a subsequent phase of plagioclase and pyroxene crystallisation was initiated, the plagioclase grains from the previous crystallisation event had not yet completely settled. This hypothesis explains how a plagioclase slurry can penetrate pull-apart structures as proposed by Maier et al. (2016) and result in potholing (Fig. 29). In contrast, the Merensky orthopyroxenite, with HREE/LREE-enrichment and generally more enriched incompatible trace element concentrations, points to a different magmatic history involving chromite and base metal sulphides and some degree of trapped liquid. The Zr content indicates a certain amount of trapped melt within the sample.

8.3. Possible association with IRUP

It has been suggested that the Iron-Rich Ultramafic Pegmatoids (IRUP) intersected at Zondereinde Mine may be spatially related to the norite-anorthosite bodies. IRUP is transgressive and preferentially replaces norite and anorthosite layers with limited replacement of the ultramafic layers and usually terminates against chromitite layers (Reid & Basson, 2002). In the southwestern extension of Zondereinde Mine, IRUP penetrates the Merensky chromitite and Pseudoreef layers, partially and/or completely replacing the reef. The barren nature of IRUP in the study area raises questions about whether these bodies have replaced PGE-bearing lithologies, leading to significant dilution of reef grades, or whether they have replaced the norite-anorthosite bodies that have cut into the strata. Reid & Basson (2002) noted that IRUP preferentially replaces norite and anorthosite. Underground mapping and borehole logging information at Zondereinde have also indicated that the IRUP in the study area has intruded and replaced the norite-anorthosite bodies. This suggests that the IRUP postdates the development of the norite-anorthosite bodies. Furthermore, this may indicate

that the IRUP and norite-anorthosite bodies are not genetically related. Further investigation on the nature of IRUP and its relative timing is beyond the scope of this study.

8.4. Impact on PGE grade

The grade analysis has revealed that the norite and anorthosite bodies in this study significantly dilute the PGE grade. Sampling data has confirmed a substantial reduction in the face grade due to the barren norite (with grades of 0.001 g/t). The dilution from these bodies was 68% and 69% at shaft-2 and shaft-1, respectively (Figs. 27 & 28). This poses an economic challenge as it could adversely affect the overall grade in the affected parts of the southwestern extension at Zondereinde.

9. CONCLUSION AND RECOMMENDATIONS

This study aimed to examine and understand the nature of the norite and anorthosite bodies identified in the potholed Merensky Reef at the southwestern extension of Zondereinde Mine (Northam Platinum), to assess their impact on mining and the grade of the reef.

The study has identified that the norite-anorthosite bodies are erratically distributed. Textural observations and trace element geochemistry have shown similarities between the norite bodies (samples 9-10 4W and 5-10 5W-2) with the hanging wall lithology (sample HW). This suggests that the norite-anorthosite bodies are part of the layered stratigraphy from the top (mafic layers of the Merensky Cyclic Unit), cutting through the footwall units (the P2 Cyclic Unit and Upper Pseudoreef), due to late-stage solidification and structural depressions associated with potholing.

There is no evidence to suggest that the norite bodies may be associated with IRUP. However, the proximity of the bodies to IRUP suggests a similar emplacement mechanism. It has been noted that IRUP in the southwestern extension of the mine is also barren, which may be due to its preferential replacement of the norite-anorthosite bodies. Further investigation into the mineralogical and geochemical characteristics of IRUP could provide more insights into their relationship with the norite-anorthosite bodies.

The study has demonstrated that the norite-anorthosite bodies are barren and therefore significantly dilute the PGE grade where they are intersected. The milling head grade will be impacted if norite-anorthosite bodies continue to be mined and hoisted as reef rather than waste, especially in stopes where the entire face length of approximately 30 meters has been affected. The effect on the milling head grade poses a substantial economic challenge as

reduced PGE grades may affect the overall viability of mining operations.

It is recommended that more careful mapping and diamond drilling be conducted to delineate the extent of these norite-anorthosite bodies ahead of mining, to understand their distribution and impact on mining, and to distinguish them as separate pothole features, to evaluate their effect on geological losses. This may inform a different mining strategy in areas affected by these barren bodies and also assist in considering these bodies in mine planning to reduce their negative impact on grade and ensure operations remain economically viable.

This study provides insights into the geological complexity and economic challenges associated with the norite and anorthosite bodies observed at Zondereinde Mine. It is also recommended that further geological studies (including geochemical and isotopic studies) be conducted to substantially understand these bodies and provide more detailed insights into their genesis and evolution, as well as to refine mining strategies.

10. REFERENCES

Arndt, N. et al. (2005). Trace elements in the Merensky Reef and adjacent norites, Bushveld Complex, South Africa. Mineralium Deposita, Volume 40, pp. 550-575.

Becker, M., Brough, C. P., Reid, D. & Smith, D. (2011). Geometallurgical characterisation of the Merensky Reef at Northam Platinum Mine - Comparison of Normal, Pothole and Transitional reef types.

Beukes, J. J., Gauert, C. D. & Giebel, R. J. (2016). Cryptic mineral variation and PGE distribution in the Merensky Reef and discontinuous mela-gabbronoritic hanging wall ("Brown Sugar Norite" - BSN) at Two Rivers Platinum Mine, Eastern Bushveld Complex, South Africa. South African Journal of Geology, 119(1), pp. 243-272.

Cawthorn, G. R. & Walraven, F. (1998). Emplacement and Crystallization Time for the Bushveld Complex. Journal of Petrology, 39(9), pp. 1669-1687.

Cawthorn, R. G. (2015). The Bushveld Complex, South Africa. Layered Intrusions, pp. 517-587.

Cawthorn, R. G. & Ashwal, L. D. (2009). Origin of Anorthosite and Magnetite Layers in the Bushveld Complex, Constrained by Major Element Compositions of Plagioclase. Journal of Petrology, 50(9), pp. 1607-1637.

Chistyakova, S., Latypov, R. & Youlton, K. (2019). Multiple Merensky Reef of the Bushveld Complex, South Africa. Contributions to Mineralogy and Petrology, 174(26).

Eales, H. V. & Cawthorn, R. G. (1996). The Bushveld Complex. Developments in Petrology, Volume 15, pp. 181-229.

Eriksson, P. G., Hattingh, P. J. & Altermann, W. (1995). An overview of the geology of the Transvaal Sequence and Bushveld Complex, South Africa. Mineralium Deposita, Volume 30, pp. 98-111.

Hill, M., Barker, F., Hunter, D. & Knight, R. (1996). Geochemical characteristics and origin of the Lebowa granite suite, Bushveld Complex. International Geology Review, 38(3), pp. 195-227.

Hunt, E. J., Latypov, R. & Horvath, P. (2018). The Merensky Cyclic Unit, Bushveld Complex, South Africa: Reality or Myth? Minerals, 8(144), pp. 1-35.

Kinnaird, J. A. (2005). The Bushveld Large Igneous Province.

Kinnaird, J. A., Kruger, F. J. & Cawthorn, R. G. (2004). Rb-Sr and Nd-Sm isotopes in fluorite related to the granites of the Bushveld Complex. South African Journal of Geology, 107(3), pp. 413-430.

Kleemann, G. J. & Twist, D. (1989). The compositionally-zoned sheet-like granite pluton of the Bushveld Complex: evidence bearing on the nature of A-type magmatism. Journal of Petrology, 30(6), pp. 1383-1414.

Kruger, F. J. & Marsh, J. S. (1985). The mineralogy, petrology, and origin of the Merensky cyclic unit in the western Bushveld Complex. Economic Geology, 80(4), pp. 958-974.

Latypov, R., Chistyakova, S., Page, A. & Hornsey, R. (2015). Field Evidence for the In Situ Crystallization of the Merensky Reef. Journal of Petrology, 56(12), pp. 2341-2372.

Latypov, R., Chistyakova, S., Barnes, S. J. & Hunt, E. J. (2017a). Origin of Platinum Deposits in Layered Intrusions by In Situ Crystallization: Evidence from Undercutting Merensky Reef of the Bushveld Complex. Journal of Petrology, 58(4), pp. 715-762.

Latypov, R., Chistyakova, S. & Mukherjee, R. (2017b). A Novel Hypothesis for Origin of Massive Chromitites in the Bushveld Complex. Journal of Petrology, 58(10), pp. 1899-1920.

Latypov, R. et al. (2020). Monomineralic anorthosites in layered intrusions are indicators of the magma chamber replenishment by plagioclase-only-saturated melts. Scientific Reports, 10(3839).

Latypov, R. M., Heinonen, J. S. & Chistyakova, S. Y. (2022). Magmatic erosion of high-temperature-melting cumulates in the Bushveld Complex by chemical dissolution. Geosystems and Geoenvironment, 1(4).

Lenhardt, N. & Eriksson, P. G. (2012). Volcanism of the Palaeoproterozoic Bushveld Large Igneous Province: The Rooiberg Group, Kaapvaal Craton, South Africa. Precambrian Research, Volume 214, pp. 82-94.

Maier, W. D., Barnes, S. J. & Groves, D. I. (2012). The Bushveld Complex, South Africa: formation of platinum–palladium, chrome- and vanadium-rich layers via hydrodynamic sorting of a mobilized cumulate slurry in a large, relatively slowly cooling, subsiding magma chamber. Mineralium Deposita, 48(1), pp. 1-56.

Maier, W. D., Karykowski, B. T. & Yang, S.-H. (2016). Formation of transgressive anorthosite seams in the Bushveld Complex via tectonically induced mobilisation of plagioclase-rich crystal mushes. Geoscience Frontiers, Volume 7, pp. 875-889.

McDonough, W. F. & Sun, S. (1995). The composition of the Earth. Chemical Geology, Volume 120, pp. 223-253.

Mitchell, A. A., Eales, H. V. & Kruger, F. J. (1998). Magma replenishment and the significance of poikilitic textures, in the Lower Main Zone of the western Bushveld Complex, South Africa. Mineralogical Magazine, 62(4), pp. 435-450.

Mitchell, A. A., Henckel, J. & Mason-Apps, A. (2019). The Upper Critical Zone of the Rustenburg Layered Suite in the Swartklip Sector, north-western Bushveld Complex, on the farm Wilgerspruit 2JQ: I. Stratigraphy and PGE mineralization patterns. South African Journal of Geology, 122(2), pp. 117-142.

Moodley, P. (2008). Facies variation in the Merensky Reef at Bafokeng Rasimone Platinum mine. s.l., The South African Institute of Mining and Metallurgy, pp. 87-95.

Naldrett, A. et al. (2011). Genesis of the PGE-Enriched Merensky Reef and Chromitite Seams of the Bushveld Complex. Society of Economic Geology, Volume 17, pp. 235-296.

Nikitina, L. P., Babushkina, M. S. & Goncharov, A. (2016). Geochemistry of REE and HFSE in the mantle peridotite and pyroxenite xenoliths from Quaternary volcanoes of north-west Spitsbergen. s.l., s.n., pp. 26-47.

Northam Platinum Holdings Limited. (2024). Mineral Resources and Mineral Reserves Statement.

O'Connor, C. & Alexandrova, T. (2021). The Geological Occurrence, Mineralogy, and Processing by Flotation of Platinum Group Minerals (PGMs) in South Africa and Russia. Minerals, 11(1), pp. 1-15.

Osbahr, I., Oberthür, T., Klemd, R. & Josties, A. (2014). Platinum-group element distribution in base-metal sulfides of the UG2 chromitite, Bushveld Complex, South Africa - a reconnaissance study. Mineralium Deposita, Volume 49, pp. 655-665.

Prevec, S. A., Ashwal, L. D. & Mkaza, M. S. (2005). Mineral disequilibrium in the Merensky Reef, western Bushveld Complex, South Africa: New Sm-Nd isotopic evidence. Contributions to Mineralogy and Petrology, 149(3), pp. 306-315.

Reid, D. L. & Basson, I. J. (2002). Iron-rich ultramafic pegmatite replacement bodies within the Upper Critical Zone. Rustenburg Layered Suite. Northam Platinum mine, South Africa. December 66(6), pp. 895-914.

Roberts, M. D. et al. (2006). The Merensky Cyclic Unit and its impact on footwall cumulates below Normal and Regional Pothole reef types in the Western Bushveld Complex. Mineralium Deposita, 42(3), pp. 271-292.

Schoenberg, R., Kruger, J. F., Thomas, M. C. & Kramers, J. D. (1999). PGE enrichment in chromitite layers and the Merensky Reef of the western Bushveld Complex; a Re–Os and Rb–Sr isotope study. Earth and Planetary Science Letters, Volume 172, pp. 49-64.

Schouwstra, R. P., Kinloch, E. D. & Lee, C. A. (2000). A Short Geological Review of the Bushveld Complex. Platinum Metals Review, 44(1), pp. 33-39.

Scoates, J. et al. (2021). Dating the Bushveld Complex: Timing of Crystallization, Duration of Magmatism, and Cooling of the World's Largest Layered Intrusion and Related Rocks. Journal of Petrology, 62(2), pp. 1-7.

Smith, A. J. et al. (2013). Geological variations in the Merensky Reef at Bafokeng Rasimone Platinum Mine and its influence on flotation performance. Minerals Engineering, Volume 52, pp. 155-168.

Smith, D. & Basson, I. (2006). Shape and distribution analysis of Merensky Reef potholing, Northam Platinum Mine, western Bushveld Complex: Implications for pothole formation and growth. Mineraliun Deposita, 41(3), pp. 281-295.

Smith, D., Basson, I. J. & Reid, D. L. (2003). Normal reef sub-facies of Merensky reef at Northam Platinum Mine, Zwartklip facies, Western Bushveld Complex. The Canadian Mineralogist, Volume 42, pp. 243-260.

Smith, D., Basson, I. & Reid, D. (2014). Smith et al. 2002 - IAGOD - Northam Presentation [PowerPoint presentation]. Available at: https://www.researchgate.net/publication/266327387_Smith_et_al_2002_-_IAGOD_-_Northam_Presentation (Accessed: 16 September 2024).

Smith, D. S. & Basson, I. J. (2005). Shape and distribution of FWP2 potholing on the Merensky Reef, Northam Platinum Mine: Implications for pothole formation and growth.

Sun, S. & McDonough, W. F. (1989). Chemical and isotopic systematics of oceanic basalts: implications for mantle composition and processes. Geological Society, London, Volume 42, pp. 313-345.

Viljoen, M. (2016). The Bushveld Complex - Host to the World's Largest Platinum, Chromium and Vanadium Resources. Journal of International Geoscience, 39(2), pp. 238-268.

Viljoen, M. J. (1999). The nature and origin of the Merensky Reef of the western Bushveld Complex based on geological facies and geophysical data. South African Journal of Geology, 102(3), pp. 221-239.

Viring, R. G. & Cowell, M. W. (1999). The Merensky Reef on Northam Platinum Limited. South African Journal Of Geology, 102(3), pp. 192-208.

Willmore, C. C., Boudreau, A. E. & Kruger, F. J. (2000). The Halogen Geochemistry of the Bushveld Complex, Republic of South Africa: Implications for Chalcophile Element Distribution in the Lower and Critical Zones. Journal of Petrology, 41(10), pp. 1517-1539.

Wilson, A. & Chunnett, G. (2006). Trace Element and Platinum Group Element Distributions and the Genesis of the Merensky Reef, Western Bushveld Complex, South Africa. Journal of Petrology, 47(12), pp. 2369-2403.

Yudovskaya, M. A. et al. (2013). Trace-element study and age dating of zircon from chromitites of the Bushveld Complex (South Africa). Mineralogy and Petrology.

Zhou, H., Trumbull, R. B., Veksler, I. V. & Bachmann, K. (2023). The effects of iron-rich ultramafic pegmatite on the composition and mineralogy of the UG2 chromitite: a case study in the western Bushveld Complex, South Africa.